Global synchromodal transport with dynamic and stochastic shipment matching

Guo, Wenjing; Atasoy, Bilge; van Blokland, Wouter Beelaerts; Negenborn, Rudy R.

DOI
10.1016/j.tre.2021.102404

Publication date
2021

Document Version
Final published version

Published in
Transportation Research Part E: Logistics and Transportation Review

Transportation Research Part E 152 (2021) 102404

Contents lists available at ScienceDirect

Transportation Research Part E

journal homepage: www.elsevier.com/locate/tre

Global synchromodal transport with dynamic and stochastic shipment matching

Wenjing Guo [a,b,*], Bilge Atasoy [a], Wouter Beelaerts van Blokland [a], Rudy R. Negenborn [a]

[a] Department of Maritime and Transport Technology, Delft University of Technology, Mekelweg 2, 2628CD Delft, the Netherlands
[b] Department of Analytics, Operations and Information Technologies, University of Quebec at Montreal and CIRRELT, Montreal, Canada

ARTICLE INFO

Keywords:
Global synchromodal transport
Dynamic shipment matching
Spot request uncertainty
Travel time uncertainty
Hybrid stochastic approach

ABSTRACT

This paper investigates a dynamic and stochastic shipment matching problem, in which a platform aims to provide online decisions on accepting or rejecting newly received shipment requests and decisions on shipment-to-service matches in global synchromodal transportation. The problem is considered dynamic since the platform receives requests and travel times continuously in real time. The problem is considered stochastic since the information of requests and travel times is not known with certainty. To solve the problem, we develop a rolling horizon framework to handle dynamic events, a hybrid stochastic approach to address uncertainties, and a preprocessing-based heuristic algorithm to generate timely solutions at each decision epoch. The experimental results indicate that for instances with above 50% degrees of dynamism, the hybrid stochastic approach that considers shipment request and travel time uncertainties simultaneously outperforms the approaches that do not consider any uncertainty or just consider one type of uncertainties in terms of total profits, the number of infeasible transshipments, and delay in deliveries.

1. Introduction

Global container transportation is the movement of containers between inland terminals located in different continents by using ships, barges, trains, trucks or any combination of them (Yang et al., 2018). With the increasing volume of global trade, container transportation becomes more and more important in improving the efficiency of global supply chains. As the fastest-growing cargo segment, global containerized trade reached 152 million twenty-foot equivalent units (TEUs) in 2018 (UNCTAD, 2019). Traditionally, global container transportation is organized by multiple operators. For example, an inland operator in Asia transports containers from Chongqing Terminal to Shanghai Port; a shipping liner company manages the container transport from Shanghai Port to Rotterdam Port; an inland operator in Europe further transports containers from Rotterdam Port to Duisburg Terminal.

In the past decade, horizontal collaboration between shipping lines has been very popular by forming an alliance to improve the utilization of resources and increase service frequency and capacity (Lee and Song, 2017). Recently, port operators and shipping lines appear to be focusing more attention on vertical integration by expanding service networks to inland terminals, such as Maersk and

* Corresponding author at: Department of Maritime and Transport Technology, Delft University of Technology, Mekelweg 2, 2628CD Delft, the Netherlands.
E-mail addresses: guo.wenjing@courrier.uqam.ca (W. Guo), B.Atasoy@tudelft.nl (B. Atasoy), W.W.A.BeelaertsvanBlokland@tudelft.nl (W.B. van Blokland), R.R.Negenborn@tudelft.nl (R.R. Negenborn).

https://doi.org/10.1016/j.tre.2021.102404
Received 28 April 2020; Received in revised form 6 May 2021; Accepted 15 June 2021
Available online 1 July 2021

COSCO shipping Lines (UNCTAD, 2019). The vertical and horizontal collaboration among players in global container transport brings new challenges to global operators because of integrated planning in larger and more complex networks, as in Fig. 1. In such a global network, we define the global operator as the integrator that collaborates with inland carriers, ocean carriers, and terminal operators.

Apart from integrated transportation, amodal booking and differentiated fare classes have also been introduced in container transportation (van Riessen et al., 2015). Amodal booking implies that shippers do not select modes and routes for their shipments and leave the choices to a global operator. This increases the flexibility of the global operator to optimize the available capacities and to react effectively to disruptions by dynamically updating transport plans (Giusti et al., 2019). Differentiated fare classes have been proposed as incentives to promote the concept of amodal booking (van Riessen et al., 2017). For each origin–destination (OD) pair, the global operator offers multiple fare classes to shippers. A fare class is characterized by a specific price, lead time, and delay cost. Once a booking request associated with a fare class is accepted by the global operator, the transport plan that assigns specific transport services to accepted requests needs to be created.

Furthermore, digitalization and online booking platforms enabled by advanced information technologies are being increasingly used by the container industry. For example, Maersk launched an online booking platform called Maersk Spot in 2018 that allows customers to check the real-time freight rates, book ship slots online, and track their bookings (Meng et al., 2019). With Maersk Spot, the shipping company can instantly confirm whether to accept or reject a booking request and react dynamically to disturbances (e.g., service delays) by adjusting the transport plan.

The combined trend towards vertical and horizontal collaboration, amodal booking, differentiated fare classes, and digitalization gives rise to the concept of synchromodality in the container industry (van Riessen et al., 2015). Synchromodality aims to reduce transport costs, delays, and carbon emissions while improving the utilization of resources based on real-time information (Giusti et al., 2019). However, implementing synchromodality in practice is still challenging from several aspects, including pricing strategies and collaboration contracts at the strategical level, integrated service network design at the tactic level, and the allocation of resources to demands under a dynamic and stochastic environment at the operational level (Giusti et al., 2019).

In this paper, we investigate a dynamic and stochastic global shipment matching problem (DSGSM) under synchromodality. We consider a platform owned by a global operator that receives contractual and spot shipment requests from shippers and receives multimodal services from carriers. While the contractual requests are received before the planning horizon, the spot requests appear in the platform dynamically. The platform creates online decisions for shipment requests including acceptance and matching decisions in a global synchromodal network, as shown in Fig. 2. A match between a shipment and a service represents that the shipment will be transported by the service from the service's origin to the service's destination. The platform combines the matched services into shipments' itineraries. Due to spot request uncertainty and service capacity limitations, the decisions made for current requests might become suboptimal upon receiving new requests. Due to travel time uncertainty and the utilization of multimodal services, the matches made for accepted requests might become infeasible at transshipment terminals. The objective of the platform is to maximize the total profits over a given planning horizon taking into account transport costs, delays, and carbon emissions.

Thanks to the development in data analytics, probability distributions of uncertainties are often available to online platforms. While dynamic and stochastic approaches that incorporate stochastic information of random variables in online decision-making processes have been well investigated in vehicle routing problems (e.g., Ritzinger et al., 2015), resource allocation problems (e.g., Wang et al., 2017), and hinterland synchromodal transport planning problems (e.g., Guo et al., 2020a), the dynamic and stochastic approach that handles shipment request and travel time uncertainties simultaneously in global synchromodal transportation is still missing in the literature.

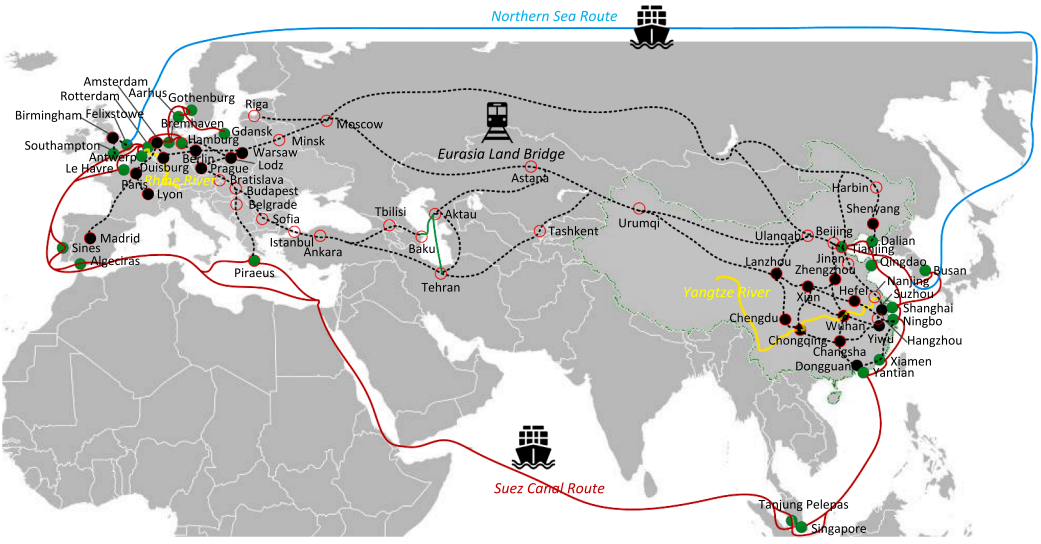

Fig. 1. Map of the integrated global network representing our vision.

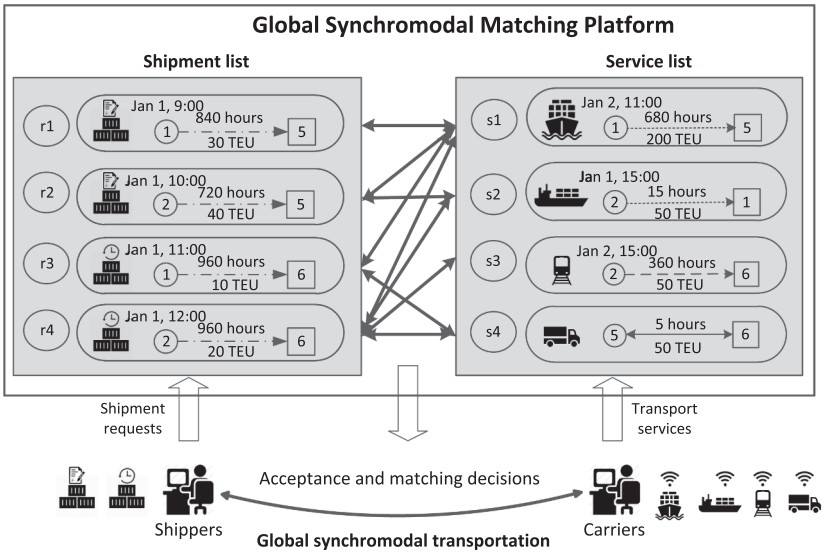

Fig. 2. Illustration of a global synchromodal matching platform.

This paper contributes to the literature in the following ways:

- We introduce the DSGSM problem for global synchromodal transport networks that integrates online acceptance and matching decisions, and considers stochastic spot requests and travel times simultaneously.
- To solve the problem, we develop a rolling horizon framework to handle dynamic events and a hybrid stochastic approach to address uncertainties. The hybrid stochastic approach consists of a sample average approximation method addressing spot request uncertainty and a chance-constrained programming method addressing travel time uncertainty. Besides, we design a preprocessing-based heuristic algorithm to generate timely solutions at each decision epoch. The methodological framework for the DSGSM problem is shown in Fig. 3.
- We evaluate the performance of the hybrid stochastic approach in comparison to the approaches that do not consider any uncertainty or only consider one type of uncertainties under a comprehensive set of experiments. The experimental results highlight the benefits of incorporating stochastic information in dynamic shipment matching processes in terms of total profits, the number of infeasible transshipments, and delay in deliveries.

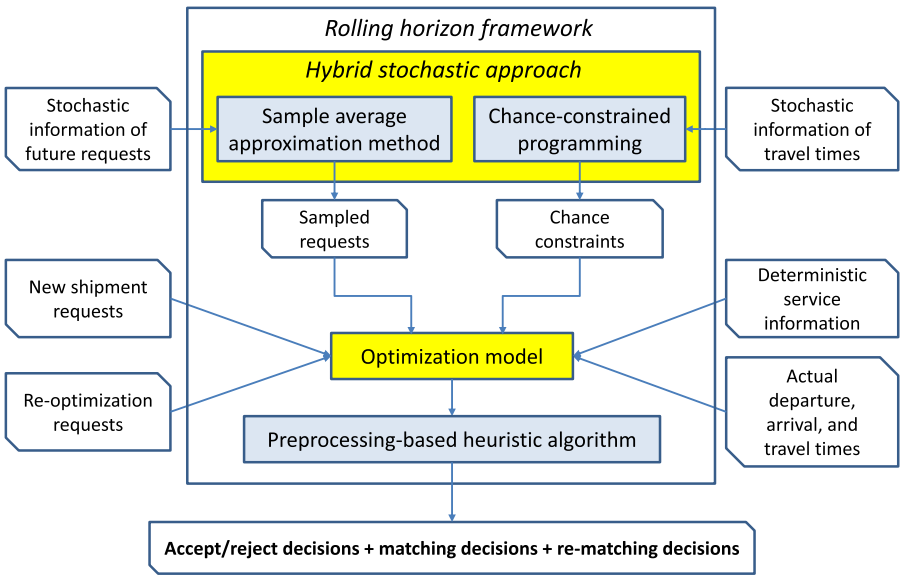

Fig. 3. Proposed methodological framework for the DSGSM problem.

Table 1
The formulation characteristics and methodologies in related literature.

Articles	Formulation characteristics									Methodologies		
	Network	Decisions	Time windows	Time schedules	Transshipment	Synchronization	Objectives	Dynamic events	Uncertainties	Dynamic approach[1]	Stochastic approach[2]	Optimization algorithm[3]
Dynamic and stochastic container booking models												
Lee et al. (2009)	Maritime (single leg)	Acceptance of bookings	-	-	-	-	Maximize revenues	Booking request	Container volume	FCFS	BL	HA
Wang (2017)	Single leg	Acceptance of bookings	-	-	-	-	Maximize profits	Booking request	Container volume, service capacity	FCFS	BL	HA
Zurheide and Fischer (2012)	Maritime	Acceptance of bookings	-	-	Y	-	Maximize profits	-	Container volume	-	BL	MILP solver
Zurheide and Fischer (2014)	Maritime	Acceptance of bookings	-	-	Y	-	Maximize profits	-	Container volume	-	BP	MILP solver
Wang (2016)	General network	Acceptance of bookings	-	-	Y	-	Maximize profits	-	Container volume, service capacity	-	SAA, PAA	IP solver
van Riessen et al. (2017)	Inland	Acceptance of bookings	-	-	Y	-	Maximize revenues	-	Container volume	-	BL	MIP solver
Bilegan et al. (2014)	Railway	Acceptance of bookings and container routing	Hard	Fixed	Y	Y	Maximize revenues	Booking request	Container volume	FCFS	SPR	MIP solver
Wang et al. (2016)	Waterway	Acceptance of bookings and container routing	Hard	Fixed	Y	Y	Maximize revenues	Booking request	Container volume	FCFS	SPR	MIP solver
Wang et al. (2017)	Inland	Acceptance of bookings	-	-	Y	-	Maximize revenues	Booking request	Container volume	BC	VFA	MIP solver
Dynamic and stochastic container routing models												
Dong et al. (2015)	Maritime	Service capacity planning and shipment routing	Hard	Fixed	Y	Y	Minimize costs	-	Container volume	-	SAA, PHA, APHA	MILP solver

(*continued on next page*)

Table 1 (*continued*)

Articles	Formulation characteristics									Methodologies		
	Network	Decisions	Time windows	Time schedules	Transshipment	Synchronization	Objectives	Dynamic events	Uncertainties	Dynamic approach[1]	Stochastic approach[2]	Optimization algorithm[3]
Dynamic and stochastic container booking models												
Demir et al. (2016)	Inland	Service schedule and shipment routing	Soft	Flexible	Y	Y	Minimize costs	-	Container volume, travel time	-	SAA	MILP solver
Li et al. (2015)	Inland	Container flow control	-	Fixed, flexible	Y	Y	Minimize costs	Container flow, travel time	-	RHF	-	HA
Qu et al. (2019)	Inland	Service schedule, shipment routing	Soft	Flexible	Y	Y	Minimize costs	Release time, container volume, travel time	-	RPP	-	MILP solver
Guo et al. (2020b)	Inland	Shipment matching	Soft	Fixed, flexible	Y	Y	Minimize costs	Shipment request	-	RHF	-	HA
van Riessen et al. (2016)	Inland	Container routing	Soft	Fixed, flexible	-	Y	Minimize costs	Container request	Container volume	FCFS	DT	MILP solver
Rivera and Mes (2017)	Inland	Assignment of freights to modes and vehicle routing	Hard	-	-	Y	Minimize costs	Shipment request	Shipment request	RP	VFA	MILP solver
Guo et al. (2020a)	Inland	Shipment matching	Soft	Fixed, flexible	Y	Y	Minimize costs	Shipment request	Shipment request	RHF	SAA	HA
Guo et al. (2020c)	Global	Acceptance of bookings and shipment matching	Soft	Fixed, flexible	Y	Y	Maximize profits	Travel time	Travel time	RHF	CCP	MILP solver
This paper	Global	Acceptance of bookings and shipment matching	Soft	Fixed, flexible	Y	Y	Maximize profits	Shipment request, travel time	Shipment request, travel time	RHF	HSP	HA

[1] FCFS: First-come-first-serve strategy; BC: Booking control strategy; RHF: Rolling horizon framework; RPP: Re-planning procedure; RP: Rollout procedures.

[2] BL: Booking limit strategy; BP: Bid-price strategy; SAA: Sample average approximation method; PAA: Progressive augmentation algorithm; SPR: Stochastic programming model with recourse; VFA: Value function approximation; PHA: Progressive hedging algorithm; APHA: Adapted progressive hedging algorithm; DT: Decision trees; CCP: Chance-constrained programming; HSA: Hybrid stochastic approach.

[3] HA: Heuristic algorithm; MILP: Mixed integer linear programming; MIP: Mixed integer programming; MINLP: Mixed integer non-linear programming.

- Although we focus on the application in global synchromodal transportation, the developed methodologies can also be applied to the more specific fields of inland and maritime transportation.

The remainder of this paper is structured as follows. We briefly review the relevant literature in Section 2. In Section 3, we provide a detailed problem description, followed by the methodology in Section 4. In Section 5, we present the experimental results. Finally, in Section 6, we provide concluding remarks and directions for future research.

2. Literature review

Global transportation consists of intercontinental transportation and inland transportation (Yang et al., 2018). In intercontinental transportation, containers are transported from export terminals to import terminals. In inland transportation, export containers are transported from inland origins to export terminals; import containers are transported from import terminals to inland destinations. While extensive studies investigated maritime transportation (Meng et al., 2014) and inland transportation (SteadieSeifi et al., 2014) in the literature, only a few studies investigated global transportation (Lee and Song, 2017). Furthermore, most of the existing global transport planning models (e.g., Meng et al., 2012; Liu et al., 2014; Tran et al., 2017; Yang et al., 2018; Wei and Dong, 2019) assumed that all the input information is static and deterministic. However, in reality, multiple dynamic events and uncertainties exist in global synchromodal transportation which highly affect the *feasibility* and *profitability* of transport plans.

In container transportation, the dynamic and stochastic models related to the DSGSM problem mainly include container booking and container routing problems. While the former considers the acceptance of booking requests to maximize revenue, the latter emphasizes the decisions on routing containers to minimize costs (Meng et al., 2014). The formulation characteristics and methodologies of dynamic and stochastic container booking and routing models are summarized in Table 1.

2.1. Dynamic and stochastic container booking models

Container booking control, also called slot allocation and capacity control, is one of the primary research topics in revenue management and is widely adopted by the airline industry (Meng et al., 2019). Container booking control aims to maximize revenue in a stochastic environment by effectively deciding on the acceptance of booking requests. According to the network structure, studies on container booking control can be divided into two groups: single-leg level and network level. While the single-leg level models (e.g., Lee et al., 2009; Wang, 2017) consider services operating on a single corridor, the network level models study services that operate on a network with the possibility of transshipments (Meng et al., 2019).

Most network container booking control models study static environments with the main strategies of booking limits and bid-price. A booking limit represents the maximum number of containers that should be allocated to a service. For example, Zurheide and Fischer (2012) proposed a slot allocation model for a liner shipping network to determine the booking limits for different booking classes (e.g. OD pair, container type, and service segment). van Riessen et al. (2017) investigated a cargo fare class mix problem in an intermodal network to maximize revenue by determining the booking limits on each fare class. Under a bid-price strategy, the decision of whether to accept or reject a booking is made based on the lowest acceptable profit value or the marginal costs for the next unit of capacity. Zurheide and Fischer (2014) developed a slot allocation model for a liner shipping company to decide the opportunity cost of a container slot as the bid-price and proved that the bid-price strategy outperforms the booking limit strategy due to the better utilization of capacity for profitable requests.

With the development of information technologies and digitalization in the container industry, researchers and industries have increasingly shifted their attention to dynamic models (Meng et al., 2019). These models can better reflect the online container booking processes and therefore better manage resource capacity. Bilegan et al. (2014) designed a load acceptance management system for rail container transport planning to dynamically accept requests or reject them in favor of future requests with potentially higher profit. Wang et al. (2016) developed a probabilistic mixed integer programming optimization model to make acceptance decisions with the objective to maximize the expected revenue of a barge carrier over a given planning horizon. Wang et al. (2017) investigated a dynamic resource allocation problem, in which an intermodal operator attempts to determine the policy that characterizes the optimal quantities of each service product allowed to be sold during each time interval within a finite selling horizon.

In comparison to the DSGSM problem proposed in this paper, the above-mentioned container booking models focus on the acceptance decisions of requests before the transport process by setting booking limits or bid-price to maximize revenue. However, we take into account the synchronization of shipments with specific time windows and services with specific time schedules during the transport process. Besides, our work considers the dynamic and stochastic information of shipment requests and travel times in a global synchromodal network, and re-optimizes the transport plan when disturbances (i.e., infeasible transshipments) happen.

2.2. Dynamic and stochastic container routing models

In the literature, container routing models have been well investigated at the strategic and tactical levels under a static context (Meng et al., 2014). Most of the studies integrate the container routing decision with other decisions such as empty container repositioning (e.g., Song and Dong, 2012) and service network design (e.g., Dong et al., 2015; Demir et al., 2016). Recently, with the increasing interest towards synchromodality, several dynamic container routing models in synchromodal transportation have been proposed. Li et al. (2015) proposed a rolling horizon approach to control and reassign container flows in an inland synchromodal freight transport network with dynamic transport demand and traffic conditions. Qu et al. (2019) proposed a mixed-integer

Table 2
Notation.

Sets:	
N	Terminals N
K	Container types, $K = \{\text{dry},\ \text{reefer}\}$
R	Shipment requests, $R = R^0 \cup R^1 \ldots \cup R^T$
R^0	Contractual requests received before the planning horizon
R^{0k}	Contractual requests received before the planning horizon with container type $k \in K$
R^t	Spot requests received during time interval $(t-1, t], t > 0$
R^{tk}	Spot requests received during time interval $(t-1, t], t > 0$ with container type $k \in K$
$\overline{R}^t$	Accepted requests that require reoptimization at decision epoch t due to infeasible transshipments, $t > 0$
$\overline{R}^{tk}$	Accepted requests that require reoptimization at decision epoch t due to infeasible transshipments, $t > 0$ with container type $k \in K$
$\omega^{\gamma h}$	Sampled requests under scenario $\gamma \in \{1, \ldots, \Gamma\}$ at stage $h \in \mathbb{H}$
$\mathbb{H}$	Prediction stages after decision epoch $t, \mathbb{H} = \{t+1, \ldots, \max\{t+H, T\}\}$
M	Modes, $M = \{\text{ship},\ \text{barge},\ \text{train},\ \text{truck}\}$
V	Set of vehicles $V = V^{\text{ship}} \cup V^{\text{barge}} \cup V^{\text{train}} \cup V^{\text{truck}}$
V^m	Vehicles with mode $m \in M$
S	Services, $S = S^{\text{ship}} \cup S^{\text{barge}} \cup S^{\text{train}} \cup S^{\text{truck}}$
S^m	Services with mode $m \in M$
S_i^+	Services departing at terminal $i \in N, S_i^+ = S_i^{+\text{ship}} \cup S_i^{+\text{barge}} \cup S_i^{+\text{train}} \cup S_i^{+\text{truck}}$
S_i^{+m}	Services departing at terminal $i \in N$ with mode $m \in M$
S_i^-	Services arriving at terminal $i \in N$, $S_i^- = S_i^{-\text{ship}} \cup S_i^{-\text{barge}} \cup S_i^{-\text{train}} \cup S_i^{-\text{truck}}$
S_i^{-m}	Services arriving at terminal $i \in N$ with mode $m \in M$
S^{+t}	Services departing at origin terminals during time interval $(t-1, t]$
S^{-t}	Services arriving at destination terminals during time interval $(t-1, t]$
Deterministic parameters	
T	Length of the planning horizon
α	Confidence level
H	Length of the prediction horizon
Γ	Number of scenarios
k_r	Container type of request $r \in R, k_r \in K$
o_r	Origin terminal of request $r \in R, o_r \in N$
d_r	Destination terminal of request $r \in R, d_r \in N$
u_r	Container volume of request $r \in R$
a_r	Announce time of request $r \in R$
e_r	Release time of request $r \in R$
l_r	Due time of request $r \in R$
p_r	Freight rate of request $r \in R$
L_r	Lead time of request $r \in R, L_r = l_r - e_r$
c_r^{D}	Delay cost of request $r \in R$ per container per hour overdue
m_s	Mode of service $s \in S, m_s \in M$
o_s	Origin terminal of service $s \in S, o_s \in N$
d_s	Destination terminal of service $s \in S, d_s \in N$
U_s^t	Free capacity of service $s \in S$ at decision epoch t
U_s^{tk}	Free capacity of service $s \in S$ at decision epoch t for container type $k \in K$
c_s	Travel cost of service $s \in S$ per container
ε_s^k	Carbon emissions of service $s \in S$ per container with type $k \in K$
$m_v^{'}$	Mode of vehicle $v \in V$
I_v	Itinerary of vehicle $v \in V \backslash V^{\text{truck}}$
I_v^n	The n^{th} service of vehicle $v \in V \backslash V^{\text{truck}}, I_v^n \in S \backslash S^{\text{truck}}$
D_s	Scheduled departure time of service $s \in S \backslash S^{\text{truck}}$
A_s	Scheduled arrival time of service $s \in S \backslash S^{\text{truck}}$
$\overline{D}_s$	Actual departure time of service $s \in S \backslash S^{\text{truck}}$
$\overline{A}_s$	Actual arrival time of service $s \in S \backslash S^{\text{truck}}$
t_s	Estimated travel time of service $s \in S$
$\overline{t}_s$	Actual travel time of service $s \in S$
ξ_{sq}	A binary variable equal to 0 if service s is the preceding service of service q, otherwise 1
c_i^m	Loading/unloading cost per container at terminal $i \in N$ with mode $m \in M$

(*continued on next page*)

Table 2 (*continued*)

f_i^m	Loading/unloading time at terminal $i \in N$ with mode $m \in M$
c_i^{S}	Storage cost at terminal i per container per hour
c^{E}	Activity-based carbon tax charged by institutional authorities
B	A large number used for binary constraints
Random variables	
$\widetilde{t}_s$	Travel time of service $s \in S, \widetilde{t}_s \sim N(\mu_s, \sigma_s^2)$
$\widetilde{D}_s$	Departure time of service $s \in S \backslash S^{\mathrm{truck}}, \widetilde{D}_s \sim N(\mu_s^+, \sigma_s^{+2})$
$\widetilde{A}_s$	Arrival time of service $s \in S \backslash S^{\mathrm{truck}}, \widetilde{A}_s \sim N(\mu_s^-, \sigma_s^{-2})$
$\widetilde{R}^t$	Future requests received at decision epoch t. The probability distributions $\{\pi_k, \pi_o, \pi_d, \pi_u, \pi_a, \pi_e, \pi_l, \pi_p, \pi_{c^{\mathrm{D}}}\}$ are assumed known.
Variables	
y_r^t	Binary variable; 1 if request $r \in R^t$ is accepted at decision epoch t
x_{rs}^t	Binary variable; 1 if request $r \in R^t \cup \overline{R}^t$ is matched with service $s \in S$ at decision epoch t, 0 otherwise
$\widehat{y}_r^{\gamma h}$	Binary variable; 1 if sample request $r \in \omega^{\gamma h}$ is accepted at decision epoch t
$\widehat{x}_{rs}^{\gamma h}$	Binary variable; 1 if sample request $r \in \omega^{\gamma h}$ is matched with service $s \in S$ at decision epoch t, 0 otherwise
z_{rsq}^t	Binary variable; 1 if request $r \in R^t \cup \overline{R}^t$ is matched with service $s \in S, x_{rs} = 1$ and service $q \in S, x_{rq} = 1$, 0 otherwise
I_r^{R}	Itinerary of request $r \in R^t \cup \overline{R}^t$ consists of matched services
D_{rs}	Departure time of truck service $s \in S^{\mathrm{truck}}$ with request $r \in R^t \cup \overline{R}^t$
c_{ri}^{T}	Transshipment cost of request $r \in R^t \cup \overline{R}^t$ at terminal $i \in N$ per container
$\widetilde{w}_{ri}$	Storage time of request $r \in R^t \cup \overline{R}^t$ at terminal $i \in N$
$\widetilde{t}_r^{\mathrm{D}}$	Delay of request $r \in R^t \cup \overline{R}^t$ at destination terminal $d_r \in N$

programming model to reschedule services and reroute shipment flows under the framework of synchromodality when unexpected dynamic events cause deviations from original plans. Guo et al. (2020b) investigated a dynamic shipment matching problem in which a platform provides online matches between shipment requests and transport services in an inland synchromodal network.

The recent developments in information technologies and data analytics have facilitated the utilization of stochastic information in online decision-making processes (Ritzinger et al., 2015). With regards to dynamic and stochastic container routing problems, van Riessen et al. (2016) proposed a decision tree to instantaneously allocate incoming containers to inland services by analyzing the solution structure of an optimization model on historical data of transport demand. Rivera and Mes (2017) proposed an adaptive approximate dynamic programming algorithm to assign the newly arrived shipment requests to a barge or trucks incorporating the probability distributions of future requests, to achieve cost minimization over a multi-period horizon. Guo et al. (2020a) proposed an anticipatory optimization approach to create online matches between shipment requests and transport services in an inland synchromodal network by incorporating the probability distributions of future requests. Guo et al. (2020c) developed a chance-constrained programming model to address travel time uncertainty in a global synchromodal shipment matching problem.

Compared with the DSGSM problem proposed in this paper, the majority of the dynamic and stochastic container routing models focus on the routing/matching decisions for booking requests in inland networks to minimize total costs without the consideration of acceptance decisions. Furthermore, none of them consider the dynamic and stochastic shipment requests and travel times simultaneously in global synchromodal transportation.

2.3. Summary

According to the above literature review, the majority of the dynamic and stochastic container booking and routing studies focus on inland networks. In this paper, we investigate global networks that integrate inland and intercontinental transportation. Besides, most of the above-mentioned studies only consider container volume uncertainty. This paper considers that all the attributes of a shipment request are uncertain, including shipments' origin, destination, container volume, time window, and fare class. Although Rivera and Mes (2017) considered shipment request uncertainty, their model neither considers the time schedules of transport services nor the transshipment operations between different modalities. To the best of our knowledge, most related to our work are the papers of Guo et al. (2020a) that addressed shipment request uncertainty and Guo et al. (2020c) that addressed travel time uncertainty in synchromodal transportation with the consideration of re-optimization procedures when disturbances happen. However, none of them consider stochastic shipment requests and travel times simultaneously. This paper develops a hybrid stochastic approach to address shipment request and travel time uncertainties integrally in online decision-making processes under the field of global synchromodal transportation.

3. Problem description

We consider a platform owned by a global operator that receives contractual and spot shipment requests from shippers, and receives ship, barge, train, and truck services from carriers, as shown in Fig. 2. We define the global operator as the coordinator that

collaborates with shippers, carriers and terminal operators to provide integrated transport planning in a global synchromodal network. The global operator does not typically own any of the transport services used to move a shipment from its origin to its destination or any of the terminals used for transshipments. Instead, the global operator enters into contracts for transport services with carriers and for loading/unloading and storage operations with terminal operators. The contract with carriers specifies the services that are available to the global operator with specific modalities, OD pairs, time schedules, available capacities, and costs. The global operators combine these services into itineraries to provide integrated transport for shipments. The global operator publishes the fare classes for each OD pair with specified freight rates, lead times, and delay costs. Shippers choose the fare classes for their shipments based on the value and urgency of commodities. After that, they initiate requests to the platform with specific OD pairs, container volumes, time windows, and fare classes, and leaves the choices of services to the platform. The notation used in this paper is shown in Table 2.

3.1. Terminals

Let N be the set of terminals. Each terminal $i \in N$ is characterized by its loading/unloading cost c_i^m, loading/unloading time f_i^m with mode $m \in M = \{\text{ship, barge, train, truck}\}$, and storage cost per container per hour c_i^{S}. We assume terminal operators provide unlimited loading/unloading and storage capacity to the global operator.

3.2. Shipment requests

Let R be the set of requests. Each request $r \in R$ is characterized by its container type k_r (i.e., dry or reefer), origin terminal o_r, destination terminal d_r, container volume u_r, announce time a_r (i.e., the time when the platform receives the request), release time e_r (i.e., the time when the shipment is available for transport process), and fare class including freight rate p_r, lead time L_r, and delay cost c_r^{D}. The due time of request r is represented as, $l_r = e_r + L_r$. Requests R consist of two groups: contractual requests R^0 and spot requests R^t. For a contractual request $r \in R^0$, the global operator has long-term contracts with shippers. Therefore, the announce time of contractual request r is $a_r = 0$. All the information $\{k_r, o_r, d_r, u_r, e_r, l_r, p_r, c_r^{\text{D}}\}$ is known in advance. On the contrary, for a spot request $r \in R^t$, the platform receives the request from spot markets during time interval $(t-1, t]$. The information of the spot request $\{k_r, o_r, d_r, u_r, e_r, l_r, p_r, c_r^{\text{D}}\}$ is unknown before its announce time a_r. However, the probability distributions of spot requests $\{\pi_k, \pi_o, \pi_d, \pi_u, \pi_a, \pi_e, \pi_l, \pi_p, \pi_{c^{\text{D}}}\}$ are assumed to be available to the platform. In addition, shippers require their shipments to be transported as a whole, and ask to receive the transport plan as soon as possible. Besides, we do not consider cancellation of requests from shippers. The requests accepted by the platform will not be rejected in the future.

3.3. Transport services

Let S be the set of services. Each ship, barge or train service $s \in S^{\text{ship}} \cup S^{\text{barge}} \cup S^{\text{train}}$ is characterized by its mode $m_s \in M$, origin terminal o_s, destination terminal d_s, free capacity U_s^{tk} in terms of container type $k \in K = \{\text{dry, reefer}\}$ at decision epoch t, total free capacity U_s^t, scheduled departure time D_s, scheduled arrival time A_s, estimated travel time t_s, travel cost c_s, and generation of carbon emissions ε_s^k for container type k. Let $\bar{t}_s, \overline{D}_s$ and $\overline{A}_s$ be the actual travel, departure and arrival time of service s which are unknown before their realization. Moreover, different services with the same mode might be operated by the same vehicle. For two successive services operated by the same vehicle, transshipment is unnecessary at the intermediate terminal. Let ξ_{sq} be equal to 0 if services s and q are operated by the same vehicle, and service s is the preceding service of service q, 1 otherwise. Each truck service $s \in S^{\text{truck}}$ is characterized by its origin terminal o_s, destination terminal d_s, free capacity U_s^{tk} in terms of container type $k \in K$ at decision epoch t, total free capacity U_s^t, estimated travel time t_s, travel cost c_s, and generation of carbon emissions ε_s^k for container type k. Let $\bar{t}_s$ be the actual travel time of service s which is unknown before its realization. Each truck service consists of a fleet of trucks that have flexible departure times. We define D_{rs} as a variable that indicates the departure time of service $s \in S^{\text{truck}}$ with shipment $r \in R$. We assume the platform receives real-time information once a service $s \in S$ departs from or arrives to a terminal.

In practice, travel time uncertainties are quite common resulting from weather conditions and traffic congestions (Demir et al., 2016). The probability distributions of travel times are assumed to be available to the platform through the analysis of historical data and external factors. In the literature, different distributions have been used to characterize travel times, such as normal distributions (e.g., Li et al., 2010; Ehmke et al., 2015; Shi et al., 2018) and Gamma distributions (e.g., Taş et al., 2014b; Long et al., 2018). Researches on fitting continuous distributions to travel time variations tend to present inconclusive and inconsistent results due to different traffic conditions and different service areas (Rahman et al., 2018). The main objective of this paper is not to find the best fit distributions of travel times but rather to investigate the benefits of incorporating travel time uncertainty in online decision-making processes under the field of global synchromodal transportation. Thanks to the properties of normal distributions, the sum and difference between two independent normal random variables are still normal distributed. These properties are critical for checking the feasible transshipments between different services. Therefore, we assume the travel times $[\tilde{t}_s]_{\forall s \in S}$ are continuous random variables following normal distributions, and are statistically independent. Let $\tilde{t}_s \sim N(\mu_s, \sigma_s^2)$, in which μ_s is the mean travel time between terminal o_s and terminal d_s, and σ_s is the corresponding standard deviation. To avoid the generation of too small or too large values, we set fixed lower and upper bounds for the realization of travel times in experimental tests.

Due to travel time uncertainties, the actual departure and arrival time of service $s \in S$ are also uncertain. The distribution of the departure time of service s is based on the distribution of the arrival time of its preceding service; the distribution of the arrival time of

service s is based on the distributions of the departure and travel time of service s. For vehicle $v \in V \backslash V^{\text{truck}}$, we define the itinerary of vehicle v as the sequence of services that the vehicle operated, and define I_v^n as the n^{th} service of vehicle v. Therefore, the departure time of service $s = I_v^n$ follows normal distribution given by:

$$\widetilde{D}_s \sim N(D_{I_v^1} + \sum_{j\in\{1\ldots n-1\}} \mu_{I_v^j} + \sum_{j\in\{1\ldots n-1\}} 2f^{m_v'}_{d_{I_v^j}}, \sum_{j\in\{1\ldots n-1\}} \sigma^2_{I_v^j}),$$

where m_v' is the mode of vehicle v. We denote $\widetilde{D}_s \sim N(\mu_s^+, \sigma_s^{+2})$. Similarly, the arrival time of service $s = I_v^n$ follows normal distribution given by:

$$\widetilde{A}_s \sim N(D_{I_v^1} + \sum_{j\in\{1\ldots n\}} \mu_{I_v^j} + \sum_{j\in\{1\ldots n-1\}} 2f^{m_v'}_{d_{I_v^j}}, \sum_{j\in\{1\ldots n\}} \sigma^2_{I_v^j}).$$

We denote $\widetilde{A}_s \sim N(\mu_s^-, \sigma_s^{-2})$.

3.4. Objectives and infeasible transshipments

The objective of the platform is to maximize total profits over the planning horizon T by dynamically optimizing acceptance and matching decisions over a global synchromodal network. In practice, the first-come-first-served (FCFS) strategy has been widely adopted in the container industry (Meng et al., 2019). Under such a strategy, decisions are made based on deterministic information only. An illustrative example of online matching processes under the FCFS strategy is shown in Fig. 4. At decision epoch $t = 8$, the platform accepts request r1, and matches r1 with ship service s1 and barge service s2 which are the cheapest services. At decision epoch $t = 9$, the platform accepts request r2, and matches r2 with rail service s3 and truck service s4. At decision epoch $t = 10$, the platform receives reefer request r3 which is very profitable. However, the platform has to reject request r3 since no capacity is available. To make better decisions over the planning horizon, the platform needs to consider the stochastic information of future requests.

On the other hand, travel time uncertainty of services in a global synchromodal network may lead to infeasible transshipments in addition to the commonly studied outcome of late or early delivery at destinations (e.g., Li et al., 2010; Taş et al., 2014a; Rodrigues et al., 2019). An illustrative example is shown in Fig. 5. A shipment is planned to be transported by a train service from its origin terminal to port A, by a ship service from port A to port B, and by two barge services from port B to its destination terminal according to fixed time schedules. The outcomes of travel time uncertainty in global synchromodal transportation include late delivery at destination terminal under realization 1 which causes delayed costs, early delivery at destination terminal under realization 2 which causes storage costs, and infeasible transshipment at port B under realization 3 which requires reoptimization.

4. Methodology

Methodologies for dynamic and stochastic problems can be divided into two categories: methods based on preprocessed decisions which determine the values and policies of decision making before the execution of the transport plan, such as approximate dynamic

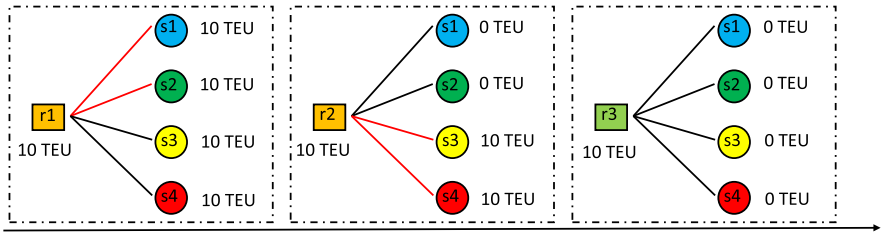

Requests	Container type	Origin	Destination	Container volume (TEU)	Announce time	Release time	Due time	Freight rate (€/TEU)	Delay cost (€/TEU-h)
r1	Dry	Shanghai	Duisburg	10	8	10	970	1800	9
r2	Dry	Shanghai	Duisburg	10	9	12	852	2400	12
r3	Reefer	Shanghai	Duisburg	10	10	12	612	3400	17

Services	Mode	Origin	Destination	Total capacity (TEU)	Reefer slots (TEU)	Departure time	Arrival time	Travel time (h)	Travel cost (€)
s1	Ship	Shanghai	Rotterdam	10	10	20	750	730	1000
s2	Barge	Rotterdam	Duisburg	10	10	800	817	17	50
s3	Train	Chongqing	Duisburg	10	10	240	600	360	2000
s4	Truck	Shanghai	Chongqing	10	10			22	1800

Fig. 4. Illustrative example of online matching processes under the FCFS strategy.

programming; and methods based on online decisions which focus on the computation when a dynamic event occurs with respect to the current system state and the available stochastic information, such as rolling horizon approaches (Ritzinger et al., 2015). The methodology proposed for the DSGSM problem belongs to the class of online decision methods. The methodology consists of a rolling horizon framework (RHF) that handles dynamic events, a hybrid stochastic approach (HSA) that addresses two types of uncertainties integrally, and a preprocessing-based heuristic algorithm (P-HA) that generates timely solutions at each optimization run, as shown in Fig. 3. Specially, we use the RHF to adapt the matching platform to new states upon receiving new requests or real-time travel times; we use a chance-constrained programming method (CCP) to generate chance constraints regarding infeasible transshipments caused by travel time uncertainty; we use a sample average approximation method (SAA) to sample requests appearing in the near future. Due to the computational complexity, we adopt the P-HA to solve the optimization problem at each decision epoch.

4.1. Rolling horizon framework

RHF is known as an efficient periodic reoptimization approach that has been applied in many fields, such as routing problems (Arslan et al., 2019) and scheduling problems (Silvente et al., 2015). Compared with the FCFS strategy, the RHF can handle multiple dynamic events that appear in a system simultaneously, which is quite common in global synchromodal transport, as illustrated in

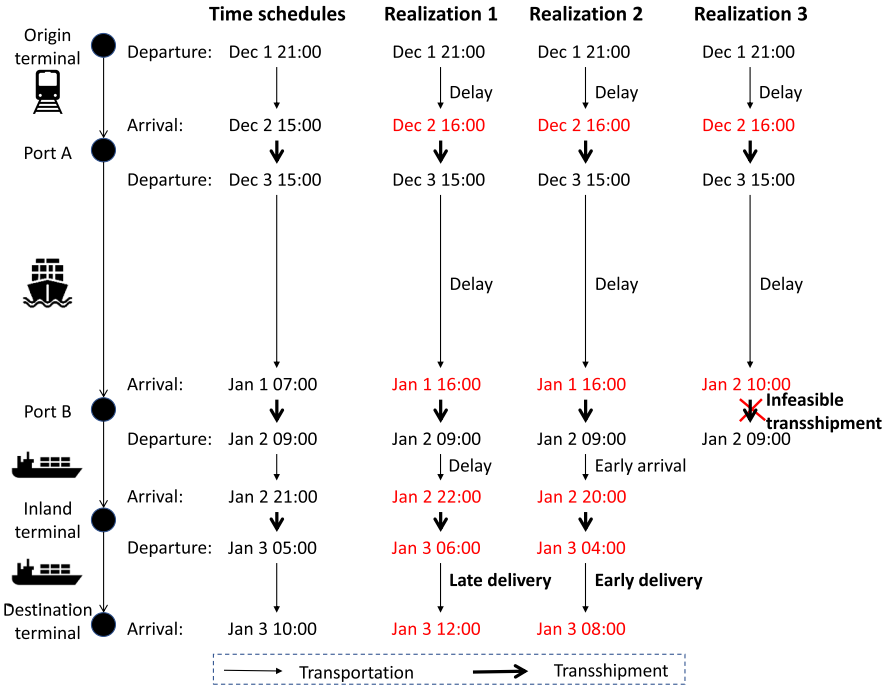

Fig. 5. Possible outcomes of travel time uncertainty in global transport.

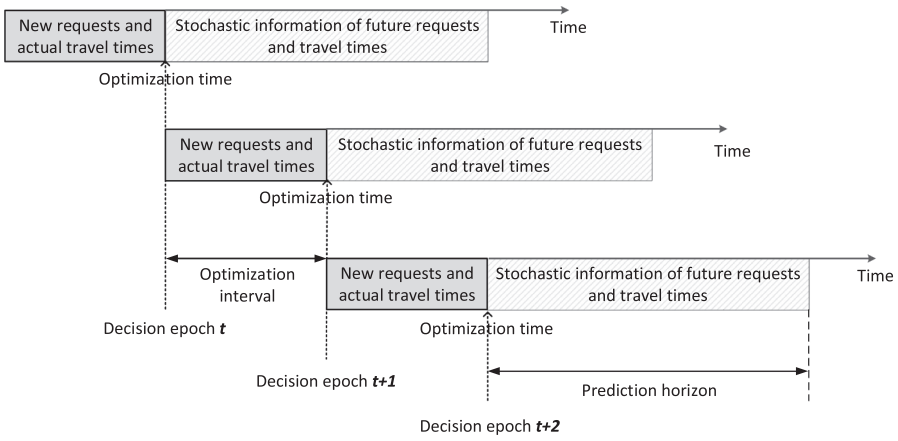

Fig. 6. Illustration of the rolling horizon framework.

Fig. 6. The RHF adapts the matching platform to new states by updating input parameters and generating reoptimization requests caused by infeasible transshipments. The pseudocode of the RHF is presented in Algorithm 1.

Algorithm 1. Rolling horizon framework.

Input: Terminals N; contractual requests R^0; services S; free capacity $\left[U_s^{0k}\right]_{\forall s\in S,k\in K}$; length of planning horizon T; probability distributions of spot requests and travel times; confidence level α; length of prediction horizon H, and number of scenarios Γ.

Output: Acceptance decision $\left[y_r^t\right]_{\forall r\in R^t,t\in\{1,\ldots,T\}}$; matching decision $\left[x_{rs}^t\right]_{\forall r\in R^t\cup\overline{R}^t,s\in S,t\in\{0,\ldots,T\}}$; itinerary $\{I_r^R\}_{r\in R}$; number of infeasible transshipments $N^{\text{infeasible}}$; actual profits $[\mathbf{AP}^t]_{t\in\{0,\ldots,T\}}$.

Initialize: Let $R^t\leftarrow\varnothing,\overline{R}^t\leftarrow\varnothing,U_s^t\leftarrow 0,I_r^R\leftarrow\varnothing,N^{\text{infeasible}}\leftarrow 0,\mathbf{AP}^t\leftarrow 0$.

1: **for** decision epoch $t\in\{0,1,\ldots,T\}$
2: receive requests R^t, actual departure time $\overline{D}_s$ of service $s\in S^{+t}\backslash S^{\text{truck}}$, actual arrival time $\overline{A}_s$ of service $s\in S^{-t}\backslash S^{\text{truck}}$, actual departure time $\overline{D}_{rs}$ of service $s\in S^{+t}\cap S^{\text{truck}}$, and actual arrival time $\overline{A}_{rs}$ of service $s\in S^{-t}\cap S^{\text{truck}}$
3: **for** request $r\in R^0\cup\ldots\cup R^{t-1}$ **do**
4: **if** $I_r^R=\varnothing$ **then**
5: go to $r=r+1$ 6: **else**
7: **for** terminal $i\in N$ **do**
8: **if** request r just arrived terminal i, service $s\in\{S^{+1}\cup\ldots\cup S^{+t}|o_s=i\}$ has already departed; or request r has already arrived terminal i, service $s\in\{S^{+t}|o_s=i\}$ just departed, but the time for transshipment operations is not enough **then**
9: update reoptimization requests $\overline{R}^t\leftarrow\overline{R}^t\cup\{r\}$
10: update number of infeasible transshipments $N^{\text{infeasible}}\leftarrow N^{\text{infeasible}}+1$
11: update free capacity $U_s^t\leftarrow U_s^t+u_r$ for $s\in\{I_r^R|D_s>t\}$
12: **if** $k_r=$ reefer **then**
13: update free capacity $U_s^{tk}\leftarrow U_s^{tk}+u_r$ for $s\in\{I_r^R|D_s>t\},k=$ reefer
14: get optimization model $\leftarrow$ ***HSA***
15: obtain acceptance and matching decision $[y^t,x^t]\leftarrow$ ***P-HA***
16: update free capacity $U_s^{t+1}\leftarrow U_s^t-\sum_{r\in R^t\cup\overline{R}^t}u_r x_{rs}^t$ for $s\in S$
17: update free capacity $U_s^{(t+1)k}\leftarrow U_s^{tk}-\sum_{r\in R^{tk}\cup\overline{R}^{tk}}u_r x_{rs}^t$ for $s\in S,k=$ reefer
18: update itinerary $\{I_r^R\}$ for $r\in R$
19: calculate total actual profits $\mathbf{AP}^t$ generated at decision epoch t
20: calculate the total profits over the planning horizon T

We define t as the points in time at which decisions are made under the RHF, referred to as the decision epoch. The planning horizon is divided into T consecutive time intervals. At decision epoch $t\in\{0,\ldots,T\}$, the RHF updates the new information received during time interval $(t-1,t]$, including new requests $R^t=\{r|t-1<a_r\leqslant t\}$, actual departure times $\left[\overline{D}_s\right]_{\forall s\in S^{+t}\backslash S^{\text{truck}}}$ and arrival times $\left[\overline{A}_s\right]_{\forall s\in S^{-t}\backslash S^{\text{truck}}}$ of ship, barge, and train services, and actual departure times $\left[\overline{D}_{rs}\right]_{\forall s\in S^{+t}\cap S^{\text{truck}}}$ and arrival times $\left[\overline{A}_{rs}\right]_{\forall s\in S^{-t}\cap S^{\text{truck}}}$ of truck services, where $S^{+t}=\{s\in S|t-1<\overline{D}_s/\overline{D}_{rs}\leqslant t\}$ is the set of services departing their origin terminals during time interval $(t-1,t];S^{-t}=\{s\in S|t-1<\overline{A}_s/\overline{A}_{rs}\leqslant t\}$ is the set of services arriving their destination terminals during time interval $(t-1,t]$.

We define y_r^t as the binary variable which is 1 if request $r\in R^t$ is accepted, 0 otherwise. Let x_{rs}^t be the binary variable which is 1 if request $r\in R^t\cup\overline{R}^t$ is matched with service $s\in S$, 0 otherwise. Here, $\overline{R}^t$ is the set of accepted requests that require reoptimization at decision epoch t due to infeasible transshipments. Based on the actual arrival and departure times of matched services $\{s\in S|x_{rs}=1\}$ of accepted request $r\in\{R^0\cup\ldots\cup R^{t-1}|y_r=1\}$, the RHF checks which requests need reoptimization due to infeasible transshipments. An infeasible transshipment happens in two situations: first, the accepted shipment r has just arrived terminal i, the matched service $s\in\{S^{+1}\cup\ldots\cup S^{+t}|x_{rs}=1,o_s=i\}$ has already departed; second, the accepted shipment r has already arrived terminal i, and the matched service $s\in\{S^{+t}|x_{rs}=1,o_s=i\}$ has just departed from terminal i, but the remaining time is not enough for transshipments. The platform thus cancels the capacity bookings on the matched services which depart after decision epoch t for reoptimization request $r\in\overline{R}^t$. The RHF then updates the free capacity regarding dry and reefer slots of these services.

The optimization model used at each decision epoch is developed based on the HSA (presented in Section 4.2). The RHF uses the P-HA (presented in Section 4.3) to generate acceptance and matching decisions based on the input parameters and the optimization model. The platform thus books capacities on the matched services based on the matching decisions. After that, the RHF updates free capacities of services and itineraries of requests, and calculates the actual profits $\mathbf{AP}^t$ generated at each decision epoch. At the end of the planning horizon, the RHF calculates the total actual profit generated over planning horizon T.

4.2. Hybrid stochastic approach

In this section, we develop the HSA to address uncertainties, which consists of the CCP that handles travel time uncertainty and the SAA that handles shipment request uncertainty.

4.2.1. Chance-constrained programming model

In the literature, different stochastic programming models have been developed to handle travel time uncertainty (Gendreau et al., 2016). In general, stochastic programming can be either formulated as a CCP model or a stochastic programming model with recourse

(SPR) (Li et al., 2010). While CCP models ensure the feasibility of stochastic constraints, SPR models define recourse actions to induce an expected penalty cost on objective functions. Typically, SPR models define a delay cost for late delivery, a storage cost for early delivery, and a large penalty cost for infeasible transshipments without the consideration of reoptimization after disturbances. Since the extra costs caused by reoptimization procedures at later stages are hard to estimate, we develop a CCP model to address travel time uncertainty. The CCP model does not take into account the correction costs caused by the reoptimization of requests.

Under CCP, each stochastic constraint will hold at least with probability α, where α is referred to as the confidence level provided by the platform. A high α means the matches have a low probability causing infeasible transshipments. The confidence level α also controls the problems' tightness and computational complexity. The objective is to maximize the total profits which consist of the planned profits at decision epoch t including freight rates, travel costs, transfer costs, storage costs, delay costs and carbon tax. The optimization model under the CCP at decision epoch t is:

$$\mathbf{P1}\ \max_{y^t,x^t} \sum_{r\in R^t} p_r u_r y_r^t - \left(\sum_{r\in R^t\cup\overline{R}^t}\sum_{s\in S} c_s x_{rs}^t u_r + \sum_{r\in R^t\cup\overline{R}^t}\sum_{i\in N} c_{ri}^{\mathrm{T}} u_r + \sum_{r\in R^t\cup\overline{R}^t}\sum_{i\in N} c_i^S \mathbb{E}(\widetilde{w}_{ri}) u_r + \sum_{r\in R^t\cup\overline{R}^t} c_r^{\mathrm{D}} \mathbb{E}\left(\widetilde{t}_r^{\mathrm{D}}\right) u_r + \sum_{k\in K}\sum_{r\in R^{tk}\cup\overline{R}^{tk}}\sum_{s\in S} c^{\mathrm{E}} \varepsilon_s^k x_{rs}^t u_r \right) \tag{1}$$

subject to

$$y_r^t \leqslant \sum_{s\in S_{o_r}^+} x_{rs}^t, \quad \forall r\in R^t, \tag{2}$$

$$y_r^t \leqslant \sum_{s\in S_{d_r}^-} x_{rs}^t, \quad \forall r\in R^t, \tag{3}$$

$$\sum_{s\in S_{o_r}^+} x_{rs}^t \leqslant 1, \quad \forall r\in R^t, \tag{4}$$

$$\sum_{s\in S_{d_r}^-} x_{rs}^t \leqslant 1, \quad \forall r\in R^t, \tag{5}$$

$$\sum_{s\in S_{o_r}^+} x_{rs}^t = 1, \quad \forall r\in \overline{R}^t, \tag{6}$$

$$\sum_{s\in S_{d_r}^-} x_{rs}^t = 1, \quad \forall r\in \overline{R}^t, \tag{7}$$

$$\sum_{s\in S_{o_r}^-} x_{rs}^t \leqslant 0, \quad \forall r\in R^t\cup\overline{R}^t, \tag{8}$$

$$\sum_{s\in S_{d_r}^+} x_{rs}^t \leqslant 0, \quad \forall r\in R^t\cup\overline{R}^t, \tag{9}$$

$$\sum_{s\in S_i^-} x_{rs}^t \leqslant 1, \quad \forall r\in R^t\cup\overline{R}^t, i\in N\backslash\{o_r,d_r\}, \tag{10}$$

$$\sum_{s\in S_i^+} x_{rs}^t \leqslant 1, \quad \forall r\in R^t\cup\overline{R}^t, i\in N\backslash\{o_r,d_r\}, \tag{11}$$

$$\sum_{s\in S_i^+} x_{rs}^t = \sum_{s\in S_i^-} x_{rs}^t, \quad \forall r\in R^t\cup\overline{R}^t, i\in N\backslash\{o_r,d_r\}, \tag{12}$$

$$\sum_{r\in R^t\cup\overline{R}^t} x_{rs}^t u_r \leqslant U_s^t, \quad \forall s\in S, \tag{13}$$

$$\sum_{r\in R^{tk}\cup\overline{R}^{tk}} x_{rs}^t u_r \leqslant U_s^{tk}, \quad \forall s\in S, k=\text{reefer}, \tag{14}$$

$$e_r + f_{o_r}^{m_s} \leqslant D_{rs} + B(1-x_{rs}^t), \quad \forall r\in R^t\cup\overline{R}^t, s\in S_{o_r}^{+\text{truck}}, \tag{15}$$

$$\mathrm{P}\{e_r + f_{o_r}^{m_s} \leqslant \widetilde{D}_s + B(1-x_{rs}^t)\} \geqslant \alpha, \quad \forall r\in R^t\cup\overline{R}^t, s\in S_{o_r}^+\backslash S_{o_r}^{+\text{truck}}, \tag{16}$$

$$\mathrm{P}\left\{\widetilde{A}_s + f_i^{m_s} + f_i^{m_q} \leqslant \widetilde{D}_q + B\left(1-x_{rs}^t\right) + B\left(1-x_{rq}^t\right)\right\} \geqslant \alpha, \forall r\in R^t\cup\overline{R}^t,\ i\in N\backslash\left\{o_r,d_r\right\}, s\in S_i^-\backslash S_i^{-truck}, q\in S_i^+\backslash S_i^{+truck}, \xi_{sq}=1, \tag{17}$$

$$\mathrm{P}\left\{D_{rs}+\widetilde{t}_s+f_i^{m_s}+f_i^{m_q}\leqslant\widetilde{D}_q+B\left(1-x_{rs}^t\right)+B\left(1-x_{rq}^t\right)\right\}\geqslant\alpha,\quad \forall r\in R^t\cup\overline{R}^t, i\in N\backslash\left\{o_r,d_r\right\}, s\in S_i^{-\text{truck}}, q\in S_i^+\backslash S_i^{+\text{truck}}, \tag{18}$$

$$\mathrm{P}\left\{\widetilde{A}_s+f_i^{m_s}+f_i^{m_q}\leqslant D_{rq}+B\left(1-x_{rs}^t\right)+B\left(1-x_{rq}^t\right)\right\}\geqslant\alpha,\quad \forall r\in R^t\cup\overline{R}^t, i\in N\backslash\left\{o_r,d_r\right\}, s\in S_i^-\backslash S_i^{-\text{truck}}, q\in S_i^{+\text{truck}}, \tag{19}$$

$$\mathrm{P}\left\{D_{rs}+\widetilde{t}_s+f_i^{m_s}+f_i^{m_q}\leqslant D_{rq}+B\left(1-x_{rs}^t\right)+B\left(1-x_{rq}^t\right)\right\}\geqslant\alpha,\quad \forall r\in R^t\cup\overline{R}^t, i\in N\backslash\left\{o_r,d_r\right\}, s\in S_i^{-\text{truck}}, q\in S_i^{+\text{truck}}, \tag{20}$$

$$c_{ri}^{\mathrm{T}}=\sum_{s\in S_i^+}x_{rs}^t c_i^{m_s},\quad \forall r\in R^t\cup\overline{R}^t, i=o_r, \tag{21}$$

$$c_{ri}^{\mathrm{T}}=\sum_{s\in S_i^-}x_{rs}^t c_i^{m_s},\quad \forall r\in R^t\cup\overline{R}^t, i=d_r, \tag{22}$$

$$c_{ri}^{\mathrm{T}}=\sum_{s\in S_i^+}\sum_{q\in S_i^-}\left(c_i^{m_s}+c_i^{m_q}\right)z_{rsq}^t\xi_{sq},\quad \forall r\in R^t\cup\overline{R}^t, i\in N\backslash\{o_r,d_r\}, \tag{23}$$

$$z_{rsq}^t\leqslant x_{rs}^t,\quad \forall r\in R^t\cup\overline{R}^t, s\in S, q\in S, \tag{24}$$

$$z_{rsq}^t\leqslant x_{rq}^t,\quad \forall r\in R^t\cup\overline{R}^t, s\in S, q\in S, \tag{25}$$

$$z_{rsq}^t\geqslant x_{rs}^t+x_{rq}^t-1,\quad \forall r\in R^t\cup\overline{R}^t, s\in S, q\in S, \tag{26}$$

$$\mathbb{E}(\widetilde{w}_{ro_r})\geqslant\mathbb{E}(\widetilde{D}_s)-f_{o_r}^{m_s}-e_r+B(x_{rs}^t-1),\quad \forall r\in R^t\cup\overline{R}^t, s\in S_{o_r}^+\backslash S_{o_r}^{+\text{truck}}, \tag{27}$$

$$\mathbb{E}(\widetilde{w}_{ro_r})\geqslant D_{rs}-f_{o_r}^{m_s}-e_r+B(x_{rs}^t-1),\quad \forall r\in R^t\cup\overline{R}^t, s\in S_{o_r}^{+\text{truck}}, \tag{28}$$

$$\begin{aligned}&\mathbb{E}(\widetilde{w}_{ri})\geqslant\mathbb{E}(\widetilde{D}_q)-\mathbb{E}(\widetilde{A}_s)-f_i^{m_s}-f_i^{m_q}+B(x_{rs}^t-1)+B(x_{rq}^t-1),\\&\forall r\in R^t\cup\overline{R}^t, i\in N\backslash\{o_r,d_r\}, s\in S_i^-\backslash S_i^{-\text{truck}}, q\in S_i^+\backslash S_i^{+\text{truck}},\end{aligned} \tag{29}$$

$$\mathbb{E}(\widetilde{w}_{ri})\geqslant\mathbb{E}\left(\widetilde{D}_q\right)-D_{rs}-\mathbb{E}\left(\widetilde{t}_s\right)-f_i^{m_s}-f_i^{m_q}+B\left(x_{rs}^t-1\right)+B\left(x_{rq}^t-1\right),\quad \forall r\in R^t\cup\overline{R}^t, i\in N\backslash\left\{o_r,d_r\right\}, s\in S_i^{-truck}, q\in S_i^+\backslash S_i^{+truck}, \tag{30}$$

$$\mathbb{E}(\widetilde{w}_{ri})\geqslant D_{rq}-\mathbb{E}\left(\widetilde{A}_s\right)-f_i^{m_s}-f_i^{m_q}+B\left(x_{rs}^t-1\right)+B\left(x_{rq}^t-1\right),\quad \forall r\in R^t\cup\overline{R}^t, i\in N\backslash\left\{o_r,d_r\right\}, s\in S_i^-\backslash S_i^{-truck}, q\in S_i^{+truck}, \tag{31}$$

$$\mathbb{E}(\widetilde{w}_{ri})\geqslant D_{rq}-D_{rs}-\mathbb{E}\left(\widetilde{t}_s\right)-f_i^{m_s}-f_i^{m_q}+B\left(x_{rs}^t-1\right)+B\left(x_{rq}^t-1\right),\quad \forall r\in R^t\cup\overline{R}^t, i\in N\backslash\left\{o_r,d_r\right\}, s\in S_i^{-truck}, q\in S_i^{+truck}, \tag{32}$$

$$\mathbb{E}(\widetilde{w}_{rd_r})\geqslant l_r-\mathbb{E}(\widetilde{A}_s)-f_{d_r}^{m_s}+B(x_{rs}^t-1),\quad \forall r\in R^t\cup\overline{R}^t, s\in S_{d_r}^-\backslash S_{d_r}^{-\text{truck}}, \tag{33}$$

$$\mathbb{E}(\widetilde{w}_{rd_r})\geqslant l_r-D_{rs}-\mathbb{E}(\widetilde{t}_s)-f_{d_r}^{m_s}+B(x_{rs}^t-1),\quad \forall r\in R^t\cup\overline{R}^t, s\in S_{d_r}^{-\text{truck}}, \tag{34}$$

$$\mathbb{E}(\widetilde{t}_r^{\mathrm{D}})\geqslant\mathbb{E}(\widetilde{A}_s)+f_{d_r}^{m_s}-l_r+B(x_{rs}^t-1),\quad \forall r\in R^t\cup\overline{R}^t, s\in S_{d_r}^-\backslash S_{d_r}^{-\text{truck}}, \tag{35}$$

$$\mathbb{E}(\widetilde{t}_r^{\mathrm{D}})\geqslant D_{rs}+\mathbb{E}(\widetilde{t}_s)+f_{d_r}^{m_s}-l_r+B(x_{rs}^t-1),\quad \forall r\in R^t\cup\overline{R}^t, s\in S_{d_r}^{-\text{truck}}, \tag{36}$$

where c_{ri}^{T} is the planned transfer cost of request r at terminal i; $\mathbb{E}(\widetilde{w}_{ri})$ is the estimated storage time of request r at terminal i; $\mathbb{E}\left(\widetilde{t}_r^{\mathrm{D}}\right)$ is the estimated delay in delivery of request r at destination terminal d_r; P is the probability measure; z_{rsq}^t is a binary variable which equals to 1 if request r has to transfer between service s and q, 0 otherwise; $\mathbb{E}(\widetilde{D}_s)=\mu_s^+, \mathbb{E}(\widetilde{A}_s)=\mu_s^-, \mathbb{E}(\widetilde{t}_s)=\mu_s$.

Constraints (2) and (3) ensure that new request $r\in R^t$ will not be accepted by the platform if there is no matching possibility. Constraints (4,5) ensure that at most one service transports new request $r\in R^t$ departing from its origin or arriving to its destination. Constraints (6,7) ensure that reoptimization request $r\in\overline{R}^t$ must be transported by one service departing from its origin and by one service arriving to its destination. Constraints (8)–(11) are designed to eliminate subtours of shipments' itineraries. Subtours could be formulated when services that arrive at the shipment's origin and depart from the shipment's destination are selected or when multiple services that depart from or arrive at a transshipment terminal are selected. Constraints (12) ensure flow conservation at transshipment terminals. Constraints (13) ensure that the total container volumes of requests matched with service s do not exceed its free capacity at decision epoch t. Constraints (14) ensure that the total volumes of reefer containers matched with service s cannot exceed its free capacity on reefer slots. In practice, dry containers can use reefer slots, but reefer containers cannot use dry slots (Meng et al., 2019).

Constraints (15) ensure that the departure time of service s minus loading time must be earlier than the release time of request r, if request r will be transported by service s depart its origin terminal. Here, B is a large enough number which ensures the time compatibility between shipment r and service s when binary variable x_{rs}^t equals 1, but leaves the constraints "open" if x_{rs}^t is 0. Constraints (16)–(20) ensure that the possibility of feasible transshipment at terminals will be higher than the confidence level α. Constraints (21)–(23) calculate the loading costs at origin terminals, the unloading costs at destination terminals, and the loading and unloading costs at transshipment terminals. Constraints (24)–(26) ensure that binary variable z_{rsq}^t equals 1 if $x_{rs}^t = 1$ and $x_{rq}^t = 1$, 0 otherwise. Constraints (27)–(34) calculate the storage time at origin, transshipment, and destination terminals. Constraints (35,36) calculate delay in deliveries at destination terminals.

To solve the CCP model, the traditional methods is to convert the chance constraints into their corresponding deterministic equations. Based on the properties of normal distributions, constraints (16)–(20) can be linearized as:

$$\frac{e_r + f_{o_r}^{m_s} + B\left(x_{rs}^t - 1\right) - \mu_s^+}{\sigma_s^+} \leqslant \phi^{-1}(1-\alpha), \quad \forall r \in R^t \cup \overline{R}^t, s \in S_{o_r}^+ \backslash S_{o_r}^{+\text{truck}}, \tag{37}$$

$$\frac{f_i^{m_s} + f_i^{m_q} + B(x_{rs}^t - 1) + B(x_{rq}^t - 1) - (\mu_q^+ - \mu_s^-)}{\sqrt{(\sigma_q^+)^2 + (\sigma_s^-)^2}} \leqslant \phi^{-1}(1-\alpha), \tag{38}$$

$$\forall r \in R^t \cup \overline{R}^t, i \in N \backslash \{o_r, d_r\}, s \in S_i^- \backslash S_i^{-\text{truck}}, q \in S_i^+ \backslash S_i^{+\text{truck}}, \xi_{sq} = 1,$$

$$\frac{D_{rs} + f_i^{m_s} + f_i^{m_q} + B\left(x_{rs}^t - 1\right) + B\left(x_{rq}^t - 1\right) - \left(\mu_q^+ - \mu_s\right)}{\sqrt{\left(\sigma_q^+\right)^2 + (\sigma_s)^2}} \leqslant \phi^{-1}(1-\alpha), \forall r \in R^t \cup \overline{R}^t, i \in N \backslash \left\{o_r, d_r\right\}, s \in S_i^{-\text{truck}}, q \in S_i^+ \backslash S_i^{+\text{truck}}, \tag{39}$$

$$\frac{D_{rq} - f_i^{m_s} - f_i^{m_q} + B\left(1 - x_{rs}^t\right) + B\left(1 - x_{rq}^t\right) - \mu_s^-}{\sigma_s^-} \geqslant \phi^{-1}(\alpha), \quad \forall r \in R^t \cup \overline{R}^t, i \in N \backslash \left\{o_r, d_r\right\}, s \in S_i^- \backslash S_i^{-\text{truck}}, q \in S_i^{+\text{truck}}, \tag{40}$$

$$\frac{D_{rq} - D_{rs} - f_i^{m_s} - f_i^{m_q} + B\left(1 - x_{rs}^t\right) + B\left(1 - x_{rq}^t\right) - \mu_s}{\sigma_s} \geqslant \phi^{-1}(\alpha), \quad \forall r \in R^t \cup \overline{R}^t, i \in N \backslash \left\{o_r, d_r\right\}, s \in S_i^{-\text{truck}}, q \in S_i^{+\text{truck}}, \tag{41}$$

where $\phi^{-1}(\alpha)$ is the inverse function of standardized normal distributions.

4.2.2. Sample average approximation method

Based on model **P1**, in this section, we present the SAA that samples requests which appear in the near future. At decision epoch t, a sample $\{\omega^1, \omega^2, \ldots, \omega^\gamma, \ldots, \omega^\Gamma\}$ of Γ scenarios is generated according to the probability distributions $\{\pi_k, \pi_o, \pi_d, \pi_u, \pi_a, \pi_e, \pi_l, \pi_p, \pi_{c^D}\}$ of shipment requests. Each scenario includes a prediction of spot requests arrived between stage $t+1$ and stage $t+H$, $\omega^\gamma = \{\omega^{\gamma(t+1)}, \omega^{\gamma(t+2)}, \ldots, \omega^{\gamma(t+H)}\}$. Here, H is the prediction horizon that is just long enough to obtain good decisions at decision epoch t. The expected cost in the future is approximated by the sample average function $\Gamma^{-1}\sum_{\gamma=1}^{\Gamma}$. Let $\widehat{y}_r^{\gamma h}$ be the binary variable which equals 1 if sample request $r \in \omega^{\gamma h}$ is accepted, and $\widehat{x}_{rs}^{\gamma h}$ be the binary variable which equals 1 if sample request $r \in \omega^{\gamma h}$ is matched with service $s \in S$ under scenario $\gamma \in \{1, .., \Gamma\}$ at stage $h \in \mathbb{H} = \{t+1, \ldots, \max\{T, t+H\}\}$. We define $\widehat{c}_{ri}^{\,\text{T}}$ as the transfer cost and $\widehat{\mathbb{E}}(\widetilde{w}_{ri})$ as the waiting time of sample request $r \in \omega^{\gamma h}$ at terminal i, $\widehat{\mathbb{E}}\left(\widetilde{t}_r^{\,\text{D}}\right)$ as the delay in delivery of sample request r. The optimization model of the DSGSM problem at decision epoch t changes to:

subject to constraints (2)–(12), (15), (21)–(41) for $r \in R^t \cup \overline{R}^t \cup \omega^{\gamma h}, \gamma \in \{1, \ldots, \Gamma\}, h \in \mathbb{H}$,

$$\begin{aligned}\textbf{P2} \quad \max_{y^t, x^t, \widetilde{y}, \widetilde{x}} & \sum_{r \in R^t} p_r u_r y_r^t - \left(\sum_{r \in R^t \cup \overline{R}^t} \sum_{s \in S} c_s x_{rs}^t u_r + \sum_{r \in R^t \cup \overline{R}^t} \sum_{i \in N} c_{ri}^{\text{T}} u_r + \sum_{r \in R^t \cup \overline{R}^t} \sum_{i \in N} c_i^{\text{S}} \mathbb{E}(\widetilde{w}_{ri}) u_r + \sum_{r \in R^t \cup \overline{R}^t} c_r^{\text{D}} \mathbb{E}(\widetilde{t}_r^{\,\text{D}}) u_r + \sum_{k \in K} \sum_{r \in R^{tk} \cup \overline{R}^{tk}} \sum_{s \in S} c^{\text{E}} \varepsilon_s^k x_{rs}^t u_r \right) \\ & + \frac{1}{\Gamma} \sum_{\gamma=1}^{\Gamma} \sum_{h \in \mathbb{H}} \left[\sum_{r \in \omega^{\gamma h}} p_r u_r \widehat{y}_r^{\gamma h} - \left(\sum_{r \in \omega^{\gamma h}} \sum_{s \in S} c_s \widehat{x}_{rs}^{\gamma h} u_r + \sum_{r \in \omega^{\gamma h}} \sum_{i \in N} \widehat{c}_{ri}^{\,\text{T}} u_r + \sum_{r \in \omega^{\gamma h}} \sum_{i \in N} c_i^{\text{S}} \widehat{\mathbb{E}}(\widetilde{w}_{ri}) u_r + \sum_{r \in \omega^{\gamma h}} c_r^{\text{D}} \widehat{\mathbb{E}}(\widetilde{t}_r^{\,\text{D}}) u_r + \sum_{k \in K} \sum_{r \in \omega^{\gamma hk}} \sum_{s \in S} c^{\text{E}} \varepsilon_s^k \widehat{x}_{rs}^{\gamma h} u_r \right) \right] \end{aligned} \tag{42}$$

Table 3
The methodological differences among DA, SA1, SA2, and HSA.

Approaches	Components			Default parameter settings		
	Dynamic approaches	Stochastic approaches	Optimization algorithm	Confidence level	Length of prediction horizon	Number of scenarios
DA	RHF	-	P-HA	-	-	-
SA1	RHF	CCP	P-HA	0.7	-	-
SA2	RHF	SAA	P-HA	-	12	10
HSA	RHF	CCP + SAA	P-HA	0.7	12	10

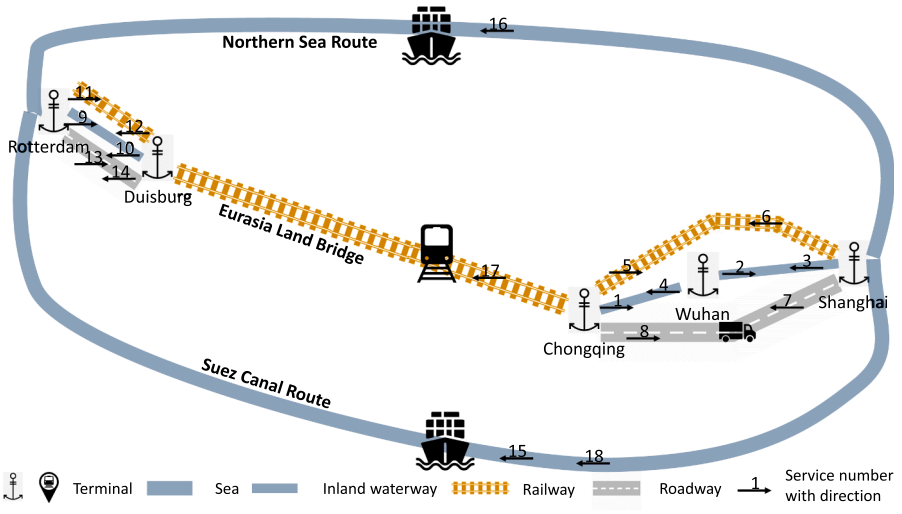

Fig. 7. The topology of global synchromodal network G1.

$$\sum\nolimits_{r\in R^t\cup\overline{R}^t} x^t_{rs}u_r + \sum_{h\in\mathbb{H}}\sum_{r\in\omega^{\gamma h}} \widehat{x}^{\gamma h}_{rs}u_r \leqslant U^t_s, \quad \forall s\in S, \gamma\in\{1,\ldots,\Gamma\}, \tag{43}$$

$$\sum\nolimits_{r\in R^{tk}\cup\overline{R}^{tk}} x^t_{rs}u_r + \sum_{h\in\mathbb{H}}\sum_{r\in\omega^{\gamma hk}} \widehat{x}^{\gamma h}_{rs}u_r \leqslant U^{tk}_s, \ \forall s\in S, k=\text{reefer}, \gamma\in\{1,\ldots,\Gamma\}. \tag{44}$$

Constraints (43,44) ensure that the total container volumes of new requests, reoptimization requests, and sample requests matched with service s do not exceed its free capacity at decision epoch t under each scenario.

4.3. Preprocessing-based heuristic algorithm

Due to the computational complexity, we design the P-HA to solve model **P2** at each decision epoch. The P-HA is adapted from the heuristic algorithm designed by Guo et al. (2020b) in which travel times are considered deterministic. The P-HA consists of three steps: preprocessing of feasible paths, preprocessing of feasible matches, and binary integer linear programming.

4.3.1. Preprocessing of feasible paths

We define a path p as a combination of services in sequence. A path p is feasible only if the services inside a combination satisfy time-spatial compatibility. Specifically, for two consecutive services s_i, s_{i+1} within path p, the destination of service s_i must be the same as the origin of service s_{i+1}; the arrival time of service s_i plus unloading time must be earlier than the departure time of service s_{i+1} minus loading time at transshipment terminal d_{s_i} with confidence level α. We define N^{path} as the largest number of services in a path. Let P denote the set of feasible paths, and P^l_{ij} represent the set of feasible paths with l services that depart from terminal i and arrive to terminal j.

The pseudocode of preprocessing of feasible paths is shown in Algorithm 2. The algorithm starts with determining the feasible paths for each OD pair with just one service, and subsequently combines these paths with a single service to create feasible paths with two services, three services, and so on. To examine whether a new path $[s_1,\ldots,s_{l-1},s]\in P^l_{ij}$ consisting of feasible path $p=[s_1,\ldots,s_{l-1}]\in P^{l-1}_{io_s}$ and service $s\in S^-_j$ is feasible, we check the transshipment feasibility between service s_{l-1} and service s by using constraints (38)–(41) with $x_{rs_{l-1}}=1, x_{rs}=1$. After that, we check whether feasible path $p\in P$ has subtours, and remove paths with subtours.

Table 4
Request data of instance G1-6-0.

Requests	Container type	Origin	Destination	Container volume (TEU)	Announce time	Release time	Lead time (h)	Freight rate (€/TEU)	Delay cost (€/TEU-h)
1	reefer	Shanghai	Rotterdam	5	0	100	720	4000	20
2	dry	Shanghai	Rotterdam	5	0	100	840	3500	17.5
3	reefer	Wuhan	Rotterdam	5	0	100	600	4500	22.5
4	dry	Wuhan	Rotterdam	5	0	100	960	3000	15
5	reefer	Chongqing	Duisburg	5	0	100	480	5000	25
6	dry	Chongqing	Duisburg	5	0	100	1080	2500	12.5

Algorithm 2. Feasible path generation algorithm.

Input: Terminals N, services S, the largest number of services in a path N^{path}, index $l \in \{1,2,\ldots,N^{\text{path}}\}$.
Output: Feasible paths $\{P_{ij}^{l}\}_{i\in N, j\in N, l\in\{1,\ldots,N^{\text{path}}\}}$.
Initialize: Let $P \leftarrow \varnothing, l \leftarrow 1$.
for terminal $i \in N$, terminal $j \in N$ **do**
  for service $s \in S$ **do**
    if origin $o_s = i$ and destination $d_s = j$ **then**
      $P_{ij}^{l} \leftarrow P_{ij}^{l} \cup \{[s]\}$
$l \leftarrow l + 1$
while $l \leqslant N^{\text{path}}$ **do**
  for terminal $i \in N$, terminal $j \in N$ **do**
    for service $s \in S$ **do**
      if origin $o_s \neq i$ and destination $d_s = j$ **then**
        for feasible path $p = [s_1, \ldots, s_{l-1}] \in P_{io_s}^{l-1}$ **do**
          if P{feasible transshipment between service s_{l-1} and s} $\geqslant \alpha$ **then**
            $P_{ij}^{l} \leftarrow P_{ij}^{l} \cup \{[s_1, \ldots, s_{l-1}, s]\}$
  $l \leftarrow l + 1$
for terminal $i \in N$, terminal $j \in N$, index $l \in \{1, \ldots, N^{\text{path}}\}$ **do**
  for path $p \in P_{ij}^{l}$ **do**
    for service $s \in p$ **do**
      if $d_s = i$ or $o_s = j$ **then**
        $P_{ij}^{l} \leftarrow P_{ij}^{l} \backslash \{p\}$
    for service $s \in p, q \in p$ **do**
      if $o_s = o_q$ **then**
        $P_{ij}^{l} \leftarrow P_{ij}^{l} \backslash \{p\}$

4.3.2. Preprocessing of feasible matches

A match between request $r \in R$ and path $p = [s_1, \ldots, s_l] \in P$ is feasible if it satisfies time-spatial compatibility. Specifically, the origin terminal of shipment request r should be the same as the origin of service s_1; the destination of request r should be the same as the destination of service s_l. The release time of request r should be earlier than the departure time of service s_1 minus loading time at origin terminal o_r with confidence level α. We denote N^{match} as the maximum number of feasible matches. Let Φ_r be the set of feasible paths for request r, and c_{rp} be the total costs of matching request r with path p including travel costs, transfer costs, storage costs, delay

Table 5
Sensitivity analysis of different policies.

Cases	Subsidies	Ice-breaking fee	IMO regulations	Itineraries					
				Request 1	Request 2	Request 3	Request 4	Request 5	Request 6
Benchmark	0	with	with	[3,4,17,10]	16	[4,17,14]	[2,15]	[]	[1,2,15,9]
1	10%	with	with	[3,4,17,10]	16	[4,17,14]	[2,15]	[]	[1,2,15,9]
2	20%	with	with	[3,4,17,10]	**[3,4,17,10]**	[4,17,14]	[2,15]	[]	[1,2,15,9]
3	30%	with	with	[3,4,17,10]	[3,4,17,10]	[4,17,14]	[2,15]	[]	[1,2,15,9]
4	40%	with	with	[3,4,17,10]	[3,4,17,10]	[4,17,14]	[2,15]	[]	**17**
5	50%	with	with	[3,4,17,10]	[3,4,17,10]	[4,17,14]	**[4,17,10]**	[]	17
6	60%	with	with	[3,4,17,10]	[3,4,17,10]	[4,17,14]	[4,17,10]	[]	17
7	70%	with	with	[3,4,17,10]	[3,4,17,10]	[4,17,14]	[4,17,10]	[]	17
8	80%	with	with	[3,4,17,10]	[3,4,17,10]	[4,17,14]	[4,17,10]	[]	17
9	90%	with	with	[3,4,17,10]	[3,4,17,10]	[4,17,14]	[4,17,10]	**17**	17
10	100%	with	with	[3,4,17,10]	[3,4,17,10]	[4,17,14]	[4,17,10]	17	17
11	0	without	with	[3,4,17,10]	16	[4,17,14]	**[2,16]**	[]	**[1,2,16,9]**
12	0	with	without	**16**	16	[4,17,14]	[2,15]	[]	[1,2,15,9]

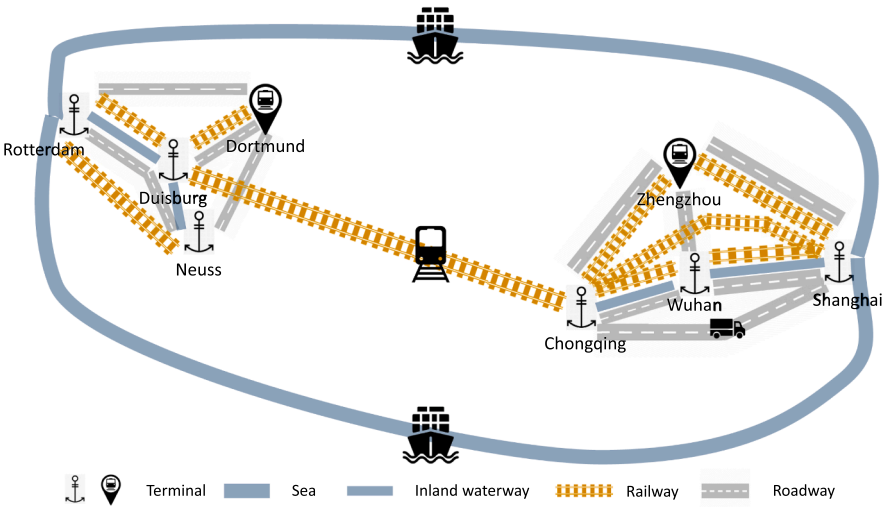

Fig. 8. The topology of global synchromodal network G2.

costs, and carbon tax.

The pseudocode of preprocessing of feasible matches is shown in Algorithm 3. For request r and path $p = [s_1, \ldots, s_l] \in P^l_{o_r d_r}$, the transshipment feasibility between r and p is checked by using constraints (15) and (37) with $x_{rs_1} = 1$. For each request r, if the number of feasible matches in Φ_r exceeds N^{match}, Φ_r will be replaced by the set of N^{match} cheapest matches.

Algorithm 3. Feasible match generation algorithm.

Input: Feasible paths P, requests $R = R^t \cup \overline{R}^t \cup \{\omega^{\gamma h}\}_{\forall \gamma \in \{1,\ldots,\Gamma\}, h \in \mathbb{H}}$, the largest number of services in a path N^{path}, maximum matches N^{match}, objective function (42).
Output: Feasible matches $\{\Phi_r\}_{\forall r \in R}$, total costs $[c_{rp}]_{\forall r \in R, p \in P}$.
Initialize: Let $\Phi \leftarrow \varnothing, l \leftarrow 1$.
for request $r \in R$ **do**
  for $l \in \{1, 2, \ldots, N^{\text{path}}\}$ **do**
    for feasible path $p = [s_1, s_2, \ldots, s_l] \in P^l_{o_r d_r}$ **do**
      if P{feasible transshipment at origin terminal o_r} $\geqslant \alpha$ **then**
        $\Phi_r \leftarrow \Phi_r \cup \{p\}$
        $c_{rp} \leftarrow$ Calculate the objective function
  if the number of feasible matches in $\Phi_r > N^{\text{match}}$ **then**
        $\Phi_r \leftarrow$ the N^{match} cheapest matches in Φ_r

4.3.3. Binary integer programming model

Based on the above preprocessing procedures, the objective function is updated to maximize the total profits for the matching of requests with feasible paths. Let z^t_{rp} be a binary variable equal to 1 if request $r \in R^t \cup \overline{R}^t$ is matched with path $p \in P$, and 0 otherwise. Let $\widehat{z}^{\gamma h}_{rp}$ be the binary variable equal to 1 if request $r \in \omega^{\gamma h}, \gamma \in \{1, \ldots, \Gamma\}, h \in \mathbb{H}$ is matched with path $p \in P$, and 0 otherwise. Model **P2** will be translated into a binary integer programming (BIP) model:

P3

$$\max_{y^t, z^t, \widehat{y}^{\gamma h}, \widehat{z}^{\gamma h}} \sum_{r \in R^t} p_r u_r y^t_r - \sum_{r \in R^t \cup \overline{R}^t} \sum_{p \in \Phi_r} c_{rp} z^t_{rp} + \frac{1}{\Gamma} \sum_{\gamma=1}^{\Gamma} \sum_{h \in \mathbb{H}} \left(\sum_{r \in \omega^{\gamma h}} p_r u_r \widehat{y}^{\gamma h}_r - \sum_{r \in \omega^{\gamma h}} \sum_{p \in \Phi_r} c_{rp} \widehat{z}^{\gamma h}_{rp} \right) \tag{45}$$

subject to

$$y^t_r \leqslant \sum_{p \in \Phi_r} z^t_{rp}, \quad \forall r \in R^t, \tag{46}$$

$$\sum_{p \in \Phi_r} z^t_{rp} \leqslant 1, \quad \forall r \in R^t, \tag{47}$$

$$\sum_{p \in \Phi_r} z^t_{rp} = 1, \quad \forall r \in \overline{R}^t, \tag{48}$$

Table 6
Probability distributions of spot requests.

Parameters	Value	Probability
Container type	{dry,reefer}	{0.9,0.1}
Origin	{Shanghai,Zhengzhou,Wuhan,Chongqing}	Uniform distribution
Destination	{Rotterdam,Duisburg,Neuss,Dortmund}	Uniform distribution
Container volume	{1,2,…,9}	Uniform distribution
$\Delta T1$	{0,1,2,…}	Poisson distribution with mean 24 min
Announce time	$a_{r+1} = a_r + \Delta T1$	
$\Delta T2$	$\{1,2,\ldots,24\}$	Uniform distribution
Release time	$e_r = \lceil a_r \rceil + \Delta T2$	
Lead time	{480,600,720,840,960,1080}	{0.15,0.15,0.2,0.2,0.15,0.15}
Freight rate	{5000,4500,4000,3500,3000,2500}	
Delay cost	{25,22.5,20,17.5,15,12.5}	

$$\widehat{y}_r^{\gamma h} \leqslant \sum_{p\in\Phi_r} \widehat{z}_{rp}^{\gamma h}, \quad \forall \gamma \in \{1,\ldots,\Gamma\}, h \in \mathbb{H}, r \in \omega^{\gamma h}, \tag{49}$$

$$\sum_{p\in\Phi_r} \widehat{z}_{rp}^{\gamma h} \leqslant 1, \quad \forall \gamma \in \{1,\ldots,\Gamma\}, h \in \mathbb{H}, r \in \omega^{\gamma h}, \tag{50}$$

$$\sum\nolimits_{r\in R^t \cup \overline{R}^t} \sum_{p\in\Phi_{rs}} u_r z_{rp}^t + \sum_{h\in\mathbb{H}} \sum_{r\in\omega^{\gamma h}} \sum_{p\in\Phi_{rs}} u_r \widehat{z}_{rp}^{\gamma h} \leqslant U_s^t, \quad \forall \gamma \in \{1,\ldots,\Gamma\}, s \in S, \tag{51}$$

$$\sum\nolimits_{r\in R^{tk} \cup \overline{R}^{tk}} \sum_{p\in\Phi_{rs}} u_r z_{rp}^t + \sum_{h\in\mathbb{H}} \sum_{r\in\omega^{\gamma hk}} \sum_{p\in\Phi_{rs}} u_r \widehat{z}_{rp}^{\gamma h} \leqslant U_s^{tk}, \quad \forall \gamma \in \left\{1,\ldots,\Gamma\right\}, s \in S, k = \text{reefer}, \tag{52}$$

where $\Phi_{rs} = \{p \in \Phi_r | s \in p\}$.

Constraints (46,47) ensure that at most one feasible path will be assigned to each new request $r \in R^t$ if r is accepted. Constraints (48) ensure that one feasible path will be assigned to each reoptimization request $r \in \overline{R}^t$. Constraints (49,50) ensure that at most one feasible path will be assigned to each sample request $r \in \omega^{\gamma h}$ if r is accepted. Constraints (51,52) ensure that the total container volumes of requests assigned to service $s \in S$ does not exceed its free capacity regarding total slots and reefer slots.

5. Numerical experiments

In this section, we evaluate the performance of the HSA on the DSGSM problem in comparison to a deterministic approach (DA) which does not consider spot request and travel time uncertainties, a stochastic approach (SA1) which only considers travel time uncertainty, and a stochastic approach (SA2) which only considers spot request uncertainty. While the DA is similar to the approach presented in Guo et al. (2020b), the SA1 is similar to the approach presented in Guo et al. (2020c) and the SA2 is similar to the approach of Guo et al. (2020a). All of the above approaches are implemented under the RHF and supported by the P-HA that generates timely solutions at each decision epoch. The methodological differences among these approaches are summarized in Table 3. The approaches are implemented in MATLAB, and all experiments are executed on 3.70 GHz Intel Xeon processors with 32 GB of RAM. The optimization problems are solved with CPLEX 12.6.3.

Unless otherwise stated, the benchmark values of coefficients are set as follows: planning horizon (unit: hours) $T = 1400$; the length of time intervals is one hour; loading cost (unit: €/TEU) $c_i^{\text{ship}} = 18, c_i^{\text{barge}} = 18, c_i^{\text{train}} = 12, c_i^{\text{truck}} = 12$ for $i \in N$; loading time (unit: hours) $f_i^{\text{ship}} = 12, f_i^{\text{barge}} = 4, f_i^{\text{train}} = 2, f_i^{\text{truck}} = 1$ for $i \in N$; storage cost (unit: €/TEU-h) $c_i^{\text{S}} = 1$ for $i \in N$; carbon tax (unit: €/kg) $c^{\text{E}} = 0.07$;

Table 7
Performance of the preprocessing-based heuristic algorithm.

Instances	Exact approach				P-HA (3, 100)		P-HA (5, 200)		P-HA (N^{path}=7, N^{match}=unlimited)			
	N.var	N.con	Obj	CPU	gaps (%)	CPU	gaps (%)	CPU	N.var	N.con	Obj	CPU
G0-5-0	2268	6540	13107	40.44	−2.06	0.16	0.00	0.24	76	46	13107	0.27
G0-10-0	3780	10840	26114	181.36	−2.74	0.17	0.00	0.24	121	52	26114	0.32
G1-1-0	11466	35994	23127	7417.06	0.00	1.23	0.00	13.03	297	53	23127	190.50
G1-10-0	114660	362164			−6.90	1.30	0.00	15.81	34613	192	62090	216.88
G1-100-0	1146600	3612428			−8.14	4.29	0.00	56.69	368430	391	545749	549.22
G1-200-0	2293200	7224988			−5.67	7.81	0.00	97.58	716098	592	1331016	929.47
G1-300-0	3439800	10846452			−4.69	16.33	−0.01	146.96	1075646	792	1889476	1563.81
G1-400-0	4586400	14439116			−2.60	26.27	0.00	212.37	1431162	991	2253709	2291.49

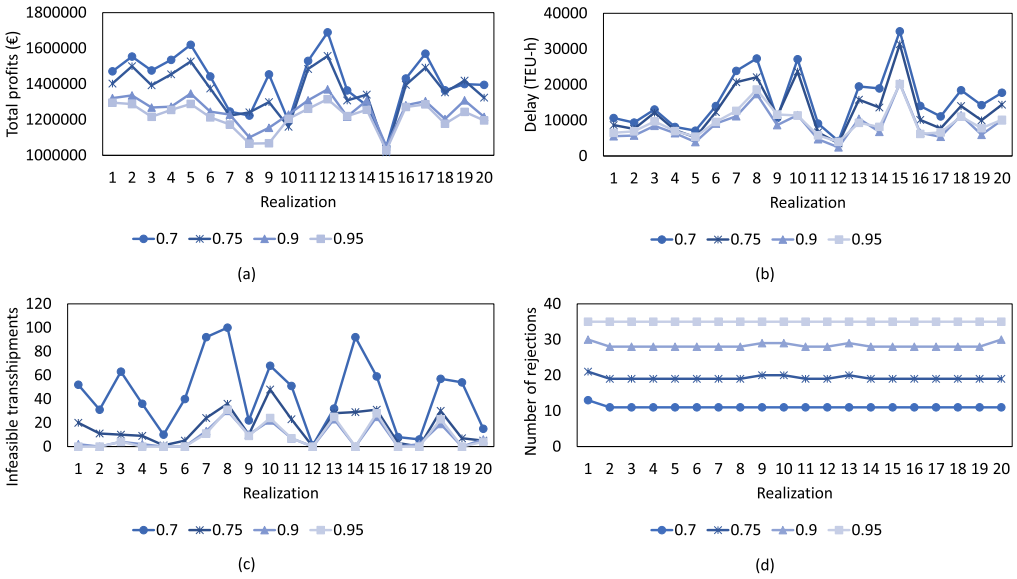

Fig. 9. The impact of different confidence levels on instance G2-150-150.

Table 8
Impact of different confidence levels on instances with different DODs.

Instances	Degree of dynamism	Confidence level	Total profits (€)	Infeasible transshipments	Rejections	CPU (seconds)	Gaps (%)
G2-225-75	25%	0.50	1443321	75	4	0.22	0.00
		0.70	1469731	45	9	0.18	**1.83**
		0.75	1434690	16	15	0.17	−0.60
		0.90	1334829	9	25	0.13	−7.52
		0.95	1271550	9	31	0.14	−11.90
G2-150-150	50%	0.50	1334025	72	6	0.43	0.00
		0.70	1413988	44	11	0.39	**5.99**
		0.75	1362974	17	19	0.36	2.17
		0.90	1253208	8	28	0.32	−6.06
		0.95	1215809	8	35	0.31	−8.86
G2-75-225	75%	0.50	1328131	77	6	0.69	0.00
		0.70	1364769	50	12	0.62	**2.76**
		0.75	1333812	18	22	0.57	0.43
		0.90	1247088	8	31	0.50	−6.10
		0.95	1214627	9	36	0.50	−8.55
G2-0-300	100%	0.50	1256014	75	20	0.96	0.00
		0.70	1276508	52	25	0.86	**1.63**
		0.75	1275004	19	28	0.86	1.51
		0.90	1263179	10	33	0.75	0.57
		0.95	1205402	10	41	0.73	−4.03

Table 9
Impact of different standard deviations.

Instances	Standard deviation coefficients (*benchmark value)	Total profits (€)	Infeasible transshipments	Rejections	Delay (TEU-h)	Gaps (%)
G2-225-75	1.0	1469731	45	9	14013	1.83
	1.5	1348739	25	19	13834	17.80
	2.0	895563	39	26	30761	**26.96**
G2-150-150	1.0	1413988	44	11	15673	5.99
	1.5	1262171	25	21	16735	19.89
	2.0	866506	35	28	31336	**42.04**
G2-75-225	1.0	1364769	50	12	16247	2.76
	1.5	1253172	27	25	16953	26.65
	2.0	866958	35	33	30925	**67.85**
G2-0-300	1.0	1276508	52	25	15388	1.63
	1.5	1220973	27	30	17437	28.61
	2.0	852891	34	37	31538	**60.61**

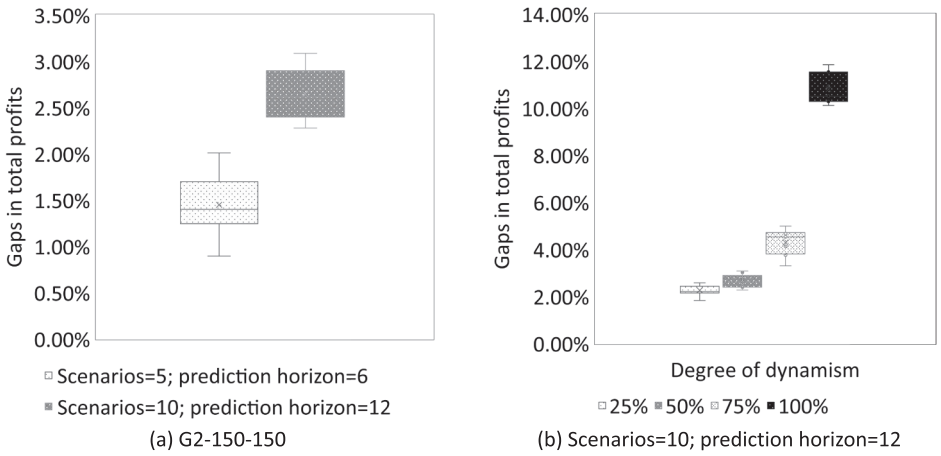

Fig. 10. Performance of the SA2 in comparison to the DA.

Table 10
Performance of the hybrid stochastic approach.

Instances	Approaches	Total profits (€)	Infeasible transshipments	Rejections	Delay (TEU-h)	Emission (kg)	CPU (seconds)	Gaps (%)
G2-225-75	DA	1443321	75	4	18026	5768862	0.22	0.00
	SA1	1469731	45	9	14013	5717070	0.18	1.83
	SA2	1476023	71	6	16824	5680165	43.22	2.27
	HSA	1459075	44	14	13531	5632343	38.24	**1.09**
G2-150-150	DA	1334025	72	6	21049	5742178	0.43	0.00
	SA1	1413988	44	11	15673	5637143	0.39	5.99
	SA2	1369395	69	11	19679	5582664	86.58	2.65
	HSA	1424060	43	15	14572	5558380	77.78	**6.75**
G2-75-225	DA	1328131	77	6	21277	5681453	0.69	0.00
	SA1	1364769	50	12	16247	5596631	0.62	2.76
	SA2	1385221	70	12	19842	5527160	334.68	4.30
	HSA	1414896	46	15	15192	5536685	175.26	**6.53**
G2-0-300	DA	1256014	75	20	19734	5408196	0.96	0.00
	SA1	1276508	52	25	15388	5222779	0.86	1.63
	SA2	1391737	70	14	19599	5455597	454.64	10.81
	HSA	1428613	47	16	15018	5486612	186.35	**13.74**

delay cost (unit: €/TEU-h) $c_r^{\mathrm{D}} = 0.005 * p_r$ for $r \in R$; mean of travel times $\mu_s = t_s$ for $s \in S$; standard deviation of travel times $\sigma_s = 0.1 * t_s$ for $s \in S \backslash S^{\mathrm{truck}}, \sigma_s = 0.5 * t_s$ for $s \in S^{\mathrm{truck}}$. Regarding the P-HA, the default settings are as follows: the largest number of services in a path $N^{\mathrm{path}} = 7$, the maximum number of feasible matches for each request $N^{\mathrm{match}} = 300$.

5.1. A small network

To test the impact of different policies in global synchromodal transport, we first consider a small network $G1$ presented by Guo et al. (2020c), as shown in Fig. 7. It consists of two terminals in Europe and three terminals in Asia that are connected by Suez Canal Route (SCR), Northern Sea Route (NSR), and Eurasia Land Bridge (ELB). Compared with the SCR, the NSR has a shorter travel time but a higher travel cost caused by ice-breaking fees (Lin and Chang, 2018). With the implementation of IMO 2020 regulations, shipping liner companies are required to use low-sulfur fuels on the sea, which in turn increases about 60% of travel costs in the SCR and the NSR (Lian et al., 2020). As an alternative, the ELB becomes more and more competitive thanks to its shortest travel time. However, without subsidies from governments, the ELB is still the most expensive route.

We use the same service data designed by Guo et al. (2020b) which consists of 18 services: 8 in Asia, 6 in Europe and 4 connecting Asia and Europe. We consider 6 contractual requests received by the system before the planning horizon. The detailed request data is shown in Table 4. Compared with reefer shipments (requests 1, 3, 5), dry shipments (requests 2, 4, 6) have longer lead times, lower freight rates, and lower delay costs.

The effects of policies are tested under instance G1-6-0 without spot request and travel time uncertainties, i.e., $\mu_s = t_s, \sigma_s = 0, \forall s \in S, R^t = \varnothing, \forall t \in \{1, \ldots, T\}$. Therefore, we set $\alpha = 0.5, H = 0, \Gamma = 0$. Under the benchmark case, the travel costs are designed under the consideration of ice-breaking fees in the NSR, IMO 2020 regulations in the SCR and the NSR, and without subsidies from governments. Table 5 shows that the itineraries of dry shipments (i.e., requests 2, 4, 6) are more sensitive to different policies than reefer shipments (i.e., requests 1, 3, 5). Under the same policy, it is obvious that reefer shipments are more likely to be assigned on the ELB

compared to dry shipments due to the time sensitivity of reefer cargoes. When government subsidies cover above 50% of ELB transport costs, all dry shipments will be switched from maritime to railway transportation. With the government subsidies and the IMO 2020 regulations, the ELB becomes more competitive in the global transport market than the SCR and the NSR. Liner shipping companies need to take actions to meet these challenges, such as adjusting sailing routes and adopting low sulfur fuel. Besides, due to the existence of the ice-breaking fee, the SCR is still more competitive than the NSR. To attract more demands on the NSR, liner shipping companies can adopt smart navigation methodologies to avoid the ice-breaking fee.

5.2. A realistic network

In this section, we test the behavior of the methodologies under a realistic network $G2$ with 8 terminals and 106 services. The hinterland-related data is adapted from Guo et al. (2020b); the intercontinental-related data is adapted from Guo et al. (2020c). The topology of network $G2$ is shown in Fig. 8. We generate several instances to represent different characteristics of requests under network $G2$. The probability distributions of spot requests are shown in Table 6. To ensure demand and supply balance, the total number of shipment requests is set to 300. We use $G2-n_1-n_2$ to represent an instance under network $G2$ with n_1 contractual requests and n_2 spot requests.

5.2.1. Performance of the P-HA

The performance of the P-HA is tested under 8 instances without dynamic events and uncertainties. The P-HA is based on pre-processing procedures which may lead to suboptimal solutions. However, when N^{path} is large enough and N^{match} is unlimited, the P-HA generates optimal solutions. We use $N^{\text{path}} = 7$ and N^{match}=unlimited as the benchmark and vary N^{path} from 3 to 7 and N^{match} from 100 to unlimited. We also report the results generated by an exact approach in which optimization model **P2** is solved by CPLEX directly. We denote 'N.var' as the number of variables, 'N.con' as the number of constraints, 'Obj' as the total profits, and 'CPU' as the computation time in seconds. We use 'gaps' to represent the gaps in total profits between the P-HA with different settings, i.e., $\text{gaps}=\frac{\text{Total profits}(N^{\text{path}},N^{\text{match}})-\text{Total profits}(7,\text{unlimited})}{\text{Total profits}(7,\text{unlimited})}$. Table 7 shows that the exact approach can only solve the first three small instances within 24 h. Increasing the largest number of services in a path to 5 and the maximum number of feasible matches to 200, the P-HA can get optimal solutions for these instances within 13.03 s. Under the same setting, the P-HA can generate 'very good' solutions within 4 min for large instances in which the largest gap is just −0.01%. By using the P-HA, the system has the flexibility to choose proper N^{path} and N^{match} values to achieve the trade-off between computational complexity and solution quality.

5.2.2. Performance of the SA1 for travel time uncertainties

In this section, we aim to investigate the performance of the SA1 in addressing travel time uncertainties under the impact of different confidence levels, degrees of dynamism, and travel time deviations.

To investigate the impact of different confidence levels, we use instance G2-150-150 under 20 realizations of travel times. The realizations of travel times are generated based on Monte Carlo Simulation by sampling their probability distributions with a fixed lower bound of $0.9 * t_s$ for $s \in S$. Fig. 9 shows that with the same confidence level, different solutions are generated under different realizations of travel times. From Fig. 9(a), we can see that on average, the SA1 has the best performance in total profits when $\alpha = 0.7$. Fig. 9(b) shows that in general, the higher the confidence level, the lower the delays in deliveries. Fig. 9(c) indicate that with a higher confidence level, the platform will choose 'suboptimal' decisions that have lower probability of infeasible transshipments. Fig. 9(d) shows that the higher the confidence level, the higher the number of rejections. Although we use profit maximization as the objective function, infeasible transshipments, delays, and rejections are also important performance indicators which reflect the platform's service level. By playing with the confidence level, decision makers can decide on how risk-averse they are and manage the trade-off between operational efficiency and service level.

To investigate the influence of confidence level on instances with different degrees of dynamism (DODs), we design the following four instances: G2-225-75, G2-150-150, G2-75-225, G2-0-300. We define DOD as the ratio between the number of spot requests and the number of total requests. We use confidence level 0.5 as the benchmark and denote 'gaps' as the gaps in total actual profits, i.e., $\text{gaps}=\frac{\text{Total profits}(\alpha)-\text{Total profits}(0.5)}{\text{Total profits}(0.5)}$. Besides, we present the average results generated under 20 realizations of travel times. Table 8 shows that for all the instances, the SA1 has the best performance in total profits with confidence level 0.7. With confidence level 0.7, the SA1 has the largest improvements in total profits under instance G2-150-150 with 50% DOD. It is also interesting to see that for all the instances, the higher the confidence level, the lower the number of infeasible transshipments and the higher the number of rejections. Furthermore, the computational complexity decreases with the increasing confidence level and increases with the increasing DOD.

To test the impact of different standard deviations of travel times, we set $\alpha = 0.7$ for the SA1 and use average results generated based on 20 realizations of actual travel times. Let 'gaps' be the gaps in total profits between the SA1 and the DA. Table 9 shows that travel time deviations have a large impact on the performance of the SA1 in increasing total profits. The larger the standard deviation, the better the performance of the SA1 in comparison to the DA. This is reasonable since with higher standard deviations, the variability in travel times is very high and the estimations are not as accurate. In comparison, instance G2-75-225 has the best performance in improving the total profits that achieves 67.85% with standard deviations $\sigma_s = 0.2 * t_s$ for $s \in S \backslash S^{\text{truck}}$ and $\sigma_s = t_s$ for $s \in S^{\text{truck}}$. Companies that have the main source of uncertainty as travel time with larger variations may benefit more from the stochastic approach SA1.

5.2.3. Performance of the SA2 for spot request uncertainties

In this section, we aim to investigate the performance of the SA2 in addressing spot request uncertainties under the impact of different numbers of scenarios (Γ) and lengths of the prediction horizon (H). We use $\Gamma = 0, H = 0$ as the benchmark. Let 'gaps in total profits' $= \frac{\text{Total profits}(\Gamma,H) - \text{Total profits}(0,0)}{\text{Total profits}(0,0)}$. Here, the total profits are the average total profits generated under 20 realizations of travel times. In case of sample requests instability, we replicate the optimization process 10 times for all instances. Fig. 10(a) shows that under instance G2-150-150, the performance of the SA2 in total profits increases as the number of scenarios and the length of the prediction horizon grow up. We set $\Gamma = 10, H = 12$ for the SA2 and use the DA as the benchmark. Fig. 10(b) shows that the SA2 outperforms the DA in all the instances, and the gap between the SA2 and the DA grows with the increasing DOD. Companies running on a larger percentage of spot requests are expected to benefit more from the stochastic approach SA2.

5.2.4. Performance of the HSA for travel time and spot request uncertainties

To investigate the benefits of incorporating the stochastic information of both travel times and spot requests, we compare the performance of the HSA with the DA, the SA1, and the SA2 under default settings. We use the DA as the benchmark and report the average results under 20 realizations of travel times and 10 samples of spot requests. We use 'gaps' to represent the gaps in total profits between different approaches, which is given by (objective value-benchmark value)/benchmark value. Table 10 shows that the HSA has better performance in total profits than the DA in all the instances and than the SA1 and SA2 in highly dynamic instances, namely above 50% DODs. On average, while the SA1 has 3.05% improvements and the SA2 has 5.01% improvements in comparison to the DA, the HSA has the largest improvements, namely 7.03%. In addition, for all the instances, the HSA generates lower infeasible transshipments and delays than other approaches. Furthermore, we notice that the number of rejections increases with the increasing DOD and achieves the highest under instance G2-0-300 which has no contractual requests. This is reasonable since the system cannot reject contractual requests. Moreover, we observe that the HSA has the best performance in instance G2-0-300 as stochastic information pays off when it is highly dynamic. Besides, it is obvious that increasing the confidence level, the computational complexity will decrease thanks to the chance constraints. However, increasing the number of scenarios and the length of the prediction horizon, the computational complexity will increase dramatically caused by the increasing size of sample requests.

5.2.5. Managerial insights

In this section, we summarize the key managerial insights derived from the above experimental results.

- Thanks to the horizontal and vertical collaboration among carriers, global operators have more flexibility to choose different routes for shipments which is critical when disturbances happen (e.g., Suez Canal blockage in March 2021). However, the increased integration in global transportation gives rise to large instances which generally cannot be solved by commercial software. Heuristic algorithms that can generate timely and high-quality solutions, like the one designed in this paper, are essential to global operators.
- Travel time uncertainty, as the main source of uncertainties in global transportation, not only affects operational efficiency but also the feasibility of transport plans. Stochastic approaches that address travel time uncertainties are critical for global operators to improve the robustness of transport plans and ensure the on-time delivery of shipments under traffic disruptions.
- Due to future request uncertainty and service capacity limitations, the capacity assigned to current requests will be unavailable for future requests which might be more profitable. Stochastic approaches that evaluate the impact of current decisions on the future state and behavior of the system play a key role in increasing the total profits of global companies over a given planning horizon.
- In practice, travel time uncertainty and shipment request uncertainty always happen simultaneously. Stochastic approaches that consider these two types of uncertainties integrally can help global companies achieve better performance in profits, feasible transshipments, and on-time deliveries in transport planning.

6. Conclusions and future research

In this paper, we investigated a dynamic and stochastic shipment matching problem in global synchromodal transportation. We considered a platform that aims to provide online acceptance and matching decisions for contractual and spot shipment requests in a global synchromodal transport network. The platform receives requests and travel times dynamically, but the probability distributions of dynamic events are available. To solve the problem, we developed a rolling horizon framework to handle dynamic events, a hybrid stochastic approach (HSA) to address shipment request and travel time uncertainties, and a preprocessing-based heuristic algorithm to generate solutions at each decision epoch.

We conducted extensive experiments to validate the performance of the HSA in comparison to the approaches that do not consider any uncertainty or only consider one type of uncertainties. The experimental results indicate that the HSA is highly effective in increasing total profits, reducing infeasible transshipments and delays on instances with a large degree of dynamism. Thanks to the flexibility of the HSA, global companies are able to adapt the transport system to their business characteristics by tuning the parameters accordingly. This way they can manage the trade-off between computational complexity and solution quality, and the trade-off between operations efficiency and service level.

This research can be extended in several directions. First, in this paper, we considered a centralized platform that provides integrated decisions for global shipments. To ensure the fairness among players, profit-sharing mechanism design is a promising research direction. Second, in practice, a large number of entities are involved in global container transport and they may not all be willing to

give authority to a centralized platform. The coordination mechanism among them and incentives to stimulate cooperation are part of future research. Third, we assumed that the platform publishes fixed fare classes for container bookings. Future research can consider dynamic pricing strategies for online platforms to realize the balance between supply and demand. Fourth, in this paper, we assumed travel times follow normal distributions, future research will be conducted to relax this restriction.

CRediT authorship contribution statement

Wenjing Guo: Conceptualization, Methodology, Software, Validation, Formal analysis, Investigation, Resources, Data curation, Writing - original draft, Writing - review & editing, Visualization. **Bilge Atasoy:** Conceptualization, Writing - review & editing, Supervision. **Wouter Beelaerts van Blokland:** Conceptualization, Supervision. **Rudy R. Negenborn:** Conceptualization, Supervision.

Acknowledgments

This research is financially supported by the China Scholarship Council under Grant 201606950003, the project “Complexity Methods for Predictive Synchromodality” (project 439.16.120) of the Netherlands Organisation for Scientific Research (NWO), and the Natural Sciences and Engineering Council of Canada (NSERC) through its Cooperative Research and Development Grants Program.

References

Arslan, A.M., Agatz, N., Kroon, L., Zuidwijk, R., 2019. Crowdsourced delivery—a dynamic pickup and delivery problem with ad hoc drivers. Transport. Sci. 53, 222–235.
Bilegan, I.C., Brotcorne, L., Feillet, D., Hayel, Y., 2014. Revenue management for rail container transportation. EURO J. Transport. Logist. 4, 261–283.
Demir, E., Burgholzer, W., Hrušovský, M., Arıkan, E., Jammernegg, W., van Woensel, T., 2016. A green intermodal service network design problem with travel time uncertainty. Transport. Res. Part B: Methodol. 93, 789–807.
Dong, J.X., Lee, C.Y., Song, D.P., 2015. Joint service capacity planning and dynamic container routing in shipping network with uncertain demands. Transport. Res. Part B: Methodol. 78, 404–421.
Ehmke, J.F., Campbell, A.M., Urban, T.L., 2015. Ensuring service levels in routing problems with time windows and stochastic travel times. Eur. J. Oper. Res. 240, 539–550.
Gendreau, M., Jabali, O., Rei, W., 2016. 50th anniversary invited article—future research directions in stochastic vehicle routing. Transport. Sci. 50, 1163–1173.
Giusti, R., Manerba, D., Bruno, G., Tadei, R., 2019. Synchromodal logistics: An overview of critical success factors, enabling technologies, and open research issues. Transport. Res. Part E: Logist. Transport. Rev. 129, 92–110.
Guo, W., Atasoy, B., van Blokland, W.B., Negenborn, R.R., 2020a. Dynamic and stochastic shipment matching problem in multimodal transportation. Transport. Res. Rec.: J. Transport. Res. Board 2674, 262–273.
Guo, W., Atasoy, B., van Blokland, W.B., Negenborn, R.R., 2020b. A dynamic shipment matching problem in hinterland synchromodal transportation. Decis. Support Syst. 113289.
Guo, W., Atasoy, B., van Blokland, W.B., Negenborn, R.R., 2020c. A global intermodal shipment matching problem under travel time uncertainty. In: Lecture Notes in Computer Science. Springer International Publishing, pp. 553–568.
Lee, C.Y., Song, D.P., 2017. Ocean container transport in global supply chains: Overview and research opportunities. Transport. Res. Part B: Methodol. 95, 442–474.
Lee, L., Chew, E., Sim, M., 2009. A revenue management model for sea cargo. Int. J. Oper. Res. 6, 195.
Li, L., Negenborn, R.R., De Schutter, B., 2015. Intermodal freight transport planning – a receding horizon control approach. Transport. Res. Part C: Emerg. Technol. 60, 77–95.
Li, X., Tian, P., Leung, S.C., 2010. Vehicle routing problems with time windows and stochastic travel and service times: Models and algorithm. Int. J. Prod. Econ. 125, 137–145.
Lian, F., He, Y., Yang, Z., 2020. Competitiveness of the china-europe railway express and liner shipping under the enforced sulfur emission control convention. Transport. Res. Part E: Logist. Transport. Rev. 135, 101861.
Lin, D.Y., Chang, Y.T., 2018. Ship routing and freight assignment problem for liner shipping: Application to the northern sea route planning problem. Transport. Res. Part E: Logist. Transport. Rev. 110, 47–70.
Liu, Z., Meng, Q., Wang, S., Sun, Z., 2014. Global intermodal liner shipping network design. Transport. Res. Part E: Logist. Transport. Rev. 61, 28–39.
Long, J., Tan, W., Szeto, W., Li, Y., 2018. Ride-sharing with travel time uncertainty. Transport. Res. Part B: Methodol. 118, 143–171.
Meng, Q., Wang, S., Andersson, H., Thun, K., 2014. Containership routing and scheduling in liner shipping: Overview and future research directions. Transport. Sci. 48, 265–280.
Meng, Q., Wang, S., Liu, Z., 2012. Network design for shipping service of large-scale intermodal liners. Transport. Res. Rec.: J. Transport. Res. Board 2269, 42–50.
Meng, Q., Zhao, H., Wang, Y., 2019. Revenue management for container liner shipping services: Critical review and future research directions. Transport. Res. Part E: Logist. Transport. Rev. 128, 280–292.
Qu, W., Rezaei, J., Maknoon, Y., Tavasszy, L., 2019. Hinterland freight transportation replanning model under the framework of synchromodality. Transport. Res. Part E: Logist. Transport. Rev. 131, 308–328.
Rahman, M.M., Wirasinghe, S., Kattan, L., 2018. Analysis of bus travel time distributions for varying horizons and real-time applications. Transport. Res. Part C: Emerg. Technol. 86, 453–466.
van Riessen, B., Negenborn, R.R., Dekker, R., 2015. Synchromodal container transportation: An overview of current topics and research opportunities. In: Lecture Notes in Computer Science. Springer International Publishing, pp. 386–397.
van Riessen, B., Negenborn, R.R., Dekker, R., 2016. Real-time container transport planning with decision trees based on offline obtained optimal solutions. Decis. Support Syst. 89, 1–16.
van Riessen, B., Negenborn, R.R., Dekker, R., 2017. The cargo fare class mix problem for an intermodal corridor: revenue management in synchromodal container transportation. Flexible Services Manuf. J. 29, 634–658.
Ritzinger, U., Puchinger, J., Hartl, R.F., 2015. A survey on dynamic and stochastic vehicle routing problems. Int. J. Prod. Res. 54, 215–231.
Rivera, A.E.P., Mes, M.R., 2017. Anticipatory freight selection in intermodal long-haul round-trips. Transport. Res. Part E: Logist. Transport. Rev. 105, 176–194.
Rodrigues, F., Agra, A., Christiansen, M., Hvattum, L.M., Requejo, C., 2019. Comparing techniques for modelling uncertainty in a maritime inventory routing problem. Eur. J. Oper. Res. 277, 831–845.
Shi, Y., Boudouh, T., Grunder, O., Wang, D., 2018. Modeling and solving simultaneous delivery and pick-up problem with stochastic travel and service times in home health care. Expert Syst. Appl. 102, 218–233.
Silvente, J., Kopanos, G.M., Pistikopoulos, E.N., Espuña, A., 2015. A rolling horizon optimization framework for the simultaneous energy supply and demand planning in microgrids. Appl. Energy 155, 485–501.
Song, D.P., Dong, J.X., 2012. Cargo routing and empty container repositioning in multiple shipping service routes. Transport. Res. Part B: Methodol. 46, 1556–1575.

SteadieSeifi, M., Dellaert, N., Nuijten, W., van Woensel, T., Raoufi, R., 2014. Multimodal freight transportation planning: A literature review. Eur. J. Oper. Res. 233, 1–15.
Taş, D., Dellaert, N., van Woensel, T., de Kok, T., 2014a. The time-dependent vehicle routing problem with soft time windows and stochastic travel times. Transport. Res. Part C: Emerg. Technol. 48, 66–83.
Taş, D., Gendreau, M., Dellaert, N., van Woensel, T., de Kok, A., 2014b. Vehicle routing with soft time windows and stochastic travel times: A column generation and branch-and-price solution approach. Eur. J. Oper. Res. 236, 789–799.
Tran, N.K., Haasis, H.D., Buer, T., 2017. Container shipping route design incorporating the costs of shipping, inland/feeder transport, inventory and CO2 emission. Maritime Econ. Logist. 19, 667–694.
UNCTAD, 2019. Review of maritime transport. URL: https://unctad.org/en/PublicationsLibrary/rmt2019_en.pdf.
Wang, H., Wang, X., Zhang, X., 2017. Dynamic resource allocation for intermodal freight transportation with network effects: Approximations and algorithms. Transport. Res. Part B: Methodol. 99, 83–112.
Wang, X., 2016. Optimal allocation of limited and random network resources to discrete stochastic demands for standardized cargo transportation networks. Transport. Res. Part B: Methodol. 91, 310–331.
Wang, X., 2017. Static and dynamic resource allocation models for single-leg transportation markets with service disruptions. Transport. Res. Part E: Logist. Transport. Rev. 103, 87–108.
Wang, Y., Bilegan, I.C., Crainic, T.G., Artiba, A., 2016. A revenue management approach for network capacity allocation of an intermodal barge transportation system. In: Lecture Notes in Computer Science. Springer International Publishing, pp. 243–257.
Wei, H., Dong, M., 2019. Import-export freight organization and optimization in the dry-port-based cross-border logistics network under the belt and road initiative. Comput. Ind. Eng. 130, 472–484.
Yang, D., Pan, K., Wang, S., 2018. On service network improvement for shipping lines under the one belt one road initiative of china. Transport. Res. Part E: Logist. Transport. Rev. 117, 82–95.
Zurheide, S., Fischer, K., 2012. A revenue management slot allocation model for liner shipping networks. Maritime Econ. Logist. 14, 334–361.
Zurheide, S., Fischer, K., 2014. Revenue management methods for the liner shipping industry. Flexible Services Manuf. J. 27, 200–223.